CHALMERS

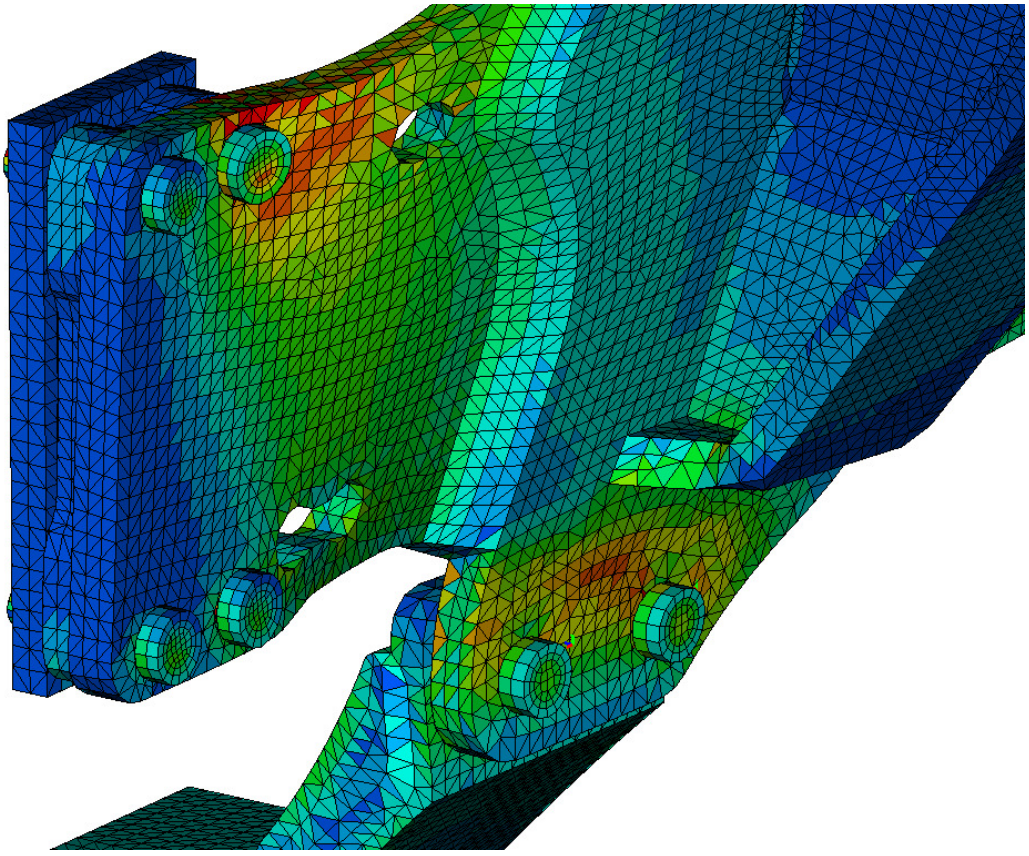

Out-of-Plane Loading Effects on Slip-Critical Screw Joints

Master's thesis in Applied Mechanics

MARCUS KARLSSON

Department of Applied Mechanics
CHALMERS UNIVERSITY OF TECHNOLOGY
Göteborg, Sweden 2016

MASTER'S THESIS IN APPLIED MECHANICS

Out-of-Plane Loading Effects on Slip-Critical Screw Joints

MARCUS KARLSSON

Department of Applied Mechanics
Division of Solid Mechanics
CHALMERS UNIVERSITY OF TECHNOLOGY
Göteborg, Sweden 2016

Out-of-Plane Loading Effects on Slip-Critical Screw Joints
MARCUS KARLSSON

Master's thesis 2016:38
ISSN 1652-8557
Department of Applied Mechanics
Division of Solid Mechanics
Chalmers University of Technology
SE-412 96 Göteborg
Sweden
Telephone: +46 (0)31-772 1000

Cover:
Bolted Joint Model

Chalmers Reproservice
Göteborg, Sweden 2016

Out-of-Plane Loading Effects on Slip-Critical Screw Joints
Master's thesis in Applied Mechanics
MARCUS KARLSSON
Department of Applied Mechanics
Division of Solid Mechanics
Chalmers University of Technology

Abstract

This thesis aims to provide a theory for the influence of out-of-plane loads on the slip condition of screw joints. This theory is developed using rigid body theory and after the forces on the plates have been found, the concept of elastic clamping areas is introduced and a formula for material stiffness developed. These expressions for the slip resistances will be used to find the critical load for a total joint slip. The theory will then be compared to a Finite Element (FE) model that is parametrised to vary the moment arm with respect to the length out of the plane.

The theory shows a very low influence of the out-of-plane load on the total slip resistance of the joint while the FE simulations show a significant increase. Using very stiff plates in the FE simulations however, yields the same results as the theory, leading the author to believe that the increased slip resistance is a geometrical effect.

The bolt forces are increased significantly in the bolts located in the area experiencing separative forces. This effect must be taken into consideration when designing joints with load applied out of the plane to avoid in-field failure due to bolts going past yield load.

Keywords: Bolted Joints, Screw Joints, Slip-Critical Applications, Bolt/Screw Joint Eccentric Loading

Preface

This is a Master's Thesis for an M.Sc. degree in Applied Mechanics at Chalmers University of Technology. The work was carried out during the spring of 2016 at the Analytics department of Alten Sweden AB for the customer Ålö. M.Sc. Mikael Almquist was the supervisor at Alten and Ph.D. Carl Sandström was the supervisor at Chalmers. Magnus Ekh, Professor at the division of Material and Computational Mechanics at Chalmers, was the examiner.

Acknowledgements

Thanks to all the colleagues at Alten for the company and support. Special thanks to Carl Sandström, my supervisor, for his support and cheerful attitude. Thanks to Mikael Almquist for giving me the opportunity to work with this project and thanks to Daniel Rickert for great discussions around mechanics and help with various software problems. I would like to thank Johan Grankvist, who has been my contact at Ålö, for his ideas and weekly followups and for the chance to visit in Umeå.

Nomenclature

α	Angle of F_{IP} to x-axis $[rad]$
Δd_b	Elongation of bolt $[m]$
Δd_c	Compression of clamped parts $[m]$
ΔF_b	Change in bolt force $[N]$
ΔF_c	Change in clamping force $[N]$
δ	Deflection $[m]$
ϵ	Kinematic strain
γ	Kinematic strain
κ	Kinematic angle
μ	Friction coefficient $[-]$
$\sigma_{bolt,i}$	Stress in bolt cross section $[N/m^2]$
σ_{fr}	Frictional stress $[N/m^2]$
$\sigma_{mean,i}$	Mean stress in bolt cross section from parallel axis theorem $[N/m^2]$
σ_n	Normal stress $[N/m^2]$
θ	Angle of material deformation frustum
d_i	Distance from centre of gravity for joint $[m]$
E	Young's modulus $[N/m^2]$
e	Eccentricity of in-plane load $[m]$
F_a	External axial load $[N]$
F_b	Tensile force in the bolt $[N]$
F_c	Clamping force between the plates $[N]$
F_s	Maximum friction force $[N]$
F_T	Transverse load $[N]$
$F_{bolt,i}$	Axial force in bolt $[N]$
F_{bs}	Friction force in bolt head plane $[N]$
F_{change}	Change in bolt and clamping force $[N]$
F_{cs}	Friction force in clamped plane $[N]$
F_{IP}	In-plane force $[N]$
$F_{mean,i}$	Force on bolt from parallel axis theorem $[N]$
F_{OP}	Axial force from external moment $[N]$
F_{pre}	Bolt pre-load force $[N]$
F_P	Transverse forces on clamped areas $[N]$
F_r	Resulting forces from in-plane forces $[N]$
i	Bolt index
$I_{par,x}$	Area moment of inertia $[m^4]$
K_b	Bolt stiffness $[N/m]$
K_c	Stiffness of clamped material $[N/m]$
K_f	Flexural stiffness $[N/m]$

k_s	Friction coefficient of faying surface
m	Number of faying surfaces (slip planes)
M_{IP}	In-plane moment $[Nm]$
M_{OP}	Out-of-plane moment $[Nm]$
n	Number of bolts
P	Critical load $[N]$
P_{avg}	Pressure $[N/m^2]$
r_0	Distance to centre of rotation $[m]$
r_i	Radial distance from assumed centre of rotation $[m]$
R_s	Kulaks slip resistance $[N]$
R_{slip}	Slip resistance $[N]$
s_{fac}	Safety factor for shear force in clamp area
T_i	Clamping force $[N]$
x_i	Bolt x-coordinate $[m]$
y	Distance from moment application $[m]$
y_i	Bolt y-coordinate $[m]$
z	Coordinate from single bolt centre of gravity $[m]$
FE	Finite Element
I.C.	Instant centre of rotation coordinate
RBE	Rigid Body Element

Contents

1 Introduction

Joining parts together using screws or bolts is an easy and common way to assemble a structure. When designing these joints it is important to know about their limit load before failure, so that unexpected failure in the field does not occur. The many failure modes of such joints make it an inherently difficult joint to analyse.

One of the challenges is to design these joints against slip, a seemingly menial task, but as the load cases become more complex, the complexity of the joint behaviour increases rapidly. One such load case is when the load is eccentrically placed out of the plane of the joint, further complexity is introduced if the load is eccentrically placed in the plane.

This thesis aims to investigate the effects on the slip condition when placing these loads eccentrically out of the plane. In Figure 1.1 a model of a tractor front loader subframe is displayed, showing how the load is applied out of the plane of the screw joints.

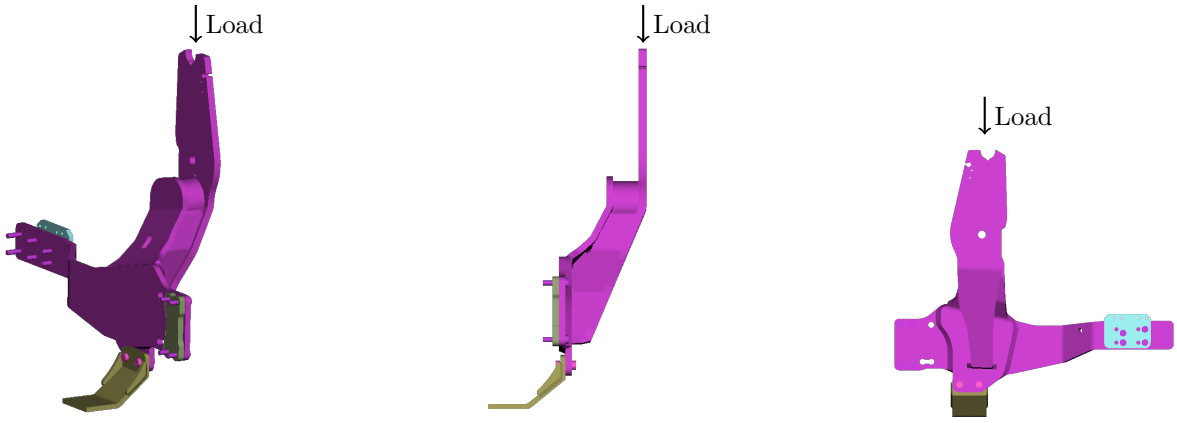

(a) *Isometric view of the model* (b) *Out-of-plane eccentricity visible* (c) *In-plane view of the joint*

Figure 1.1: *Model of tractor subframe split in symmetry plane*

FE simulation is an excellent tool in this type of analysis since regular hand calculations are not easily applicable on such a complex problem as sliding on large elastic areas.

The goal of this project is to develop a model that can incorporate an out-of-plane moment into a model to predict slipping loads. This model should be implementable in such a way that a designer can input joint data and get approximate critical load and slip conditions in the bolts.

Initially a theory using rigid bodies will be developed. This model will then be used to find the slip conditions of the joint and clamped areas.

A simplified FE model of a joint will be made to compare the results and correlate with the developed theory. The discretised model will be solved using MSC's NASTRAN solver SOL400 [1]. It is assumed that finite deformations exist due to the sliding contacts and the high loads to overcome the clamping friction of the bolts.

A model of a real joint will be compared to the theory to see if it can be applied to real world applications.

1.1 Limitations

The project will have some limitations and assumptions regarding mechanical behaviour will be made.

- Linear elastic material will be used in the FE analysis and theory
- Static conditions
- Fracture and yielding will not be considered

1.2 Review of Contact Mechanics in FEM

The theoretical model will be compared to FE simulations, where large variations can occur depending on the settings used. It is therefore important to define what settings that are used throughout the simulations.

1.2.1 Gap Function

When introducing contact mechanics, a contact function to determine when nodes are in contact is needed. The node-to-segment contact mode is chosen, meaning that the nodes will be checked against the surface of the opposing elements. The option to use segment-to-segment contact checking is possible but this function is still under development in SOL400 [2] and therefore the node-to-segment contact is used.

1.2.2 Coulomb Friction Model

The Coulomb friction model has been chosen in the FE simulations. The MSC.Nastran documentation has some notes on the constitutive equations for Coulomb friction [3]:

$$\sigma_{fr} \leq -\mu\sigma_n \tag{1.1}$$

where σ_{fr} is the frictional stress, σ_n is the normal stress ($\sigma_n \geq 0$), μ is the friction coefficient between the surfaces. In the Coulomb model, a point in contact will be either sliding or sticking.

1.2.3 Separation

Due to how nodal forces behave in 2nd order elements, the integrated nodal stress will be used as the separation condition [2] together with a tolerance. For the small testing models used in this thesis, the separation tolerance is set to 1% of the maximum contact stress in the model to achieve high accuracy. Since the separation of one node can cause another to come into contact again, it is required to set a maximum number of separations for each load step, often referred to as "chatter". After this maximum has been reached, the individual node will no longer be considered for separation. There is also a possibility to change the total number of allowed separations for all nodes in the model for a single step to further reduce chatter from node separations, limiting iterations based on the global number of node separations.

1.2.4 FE Modelling

To set up an FE simulation from a given geometry some preparations have to be made. First the geometry has to be cleaned, all surfaces defined and all volumes closed, and simplified to avoid overly complex behaviour that might not be the target of the analysis. Figure 1.2 displays a simplified flowchart of the steps needed to complete an analysis, starting from a supplied geometry and ending with the analysis of the simulated load case.

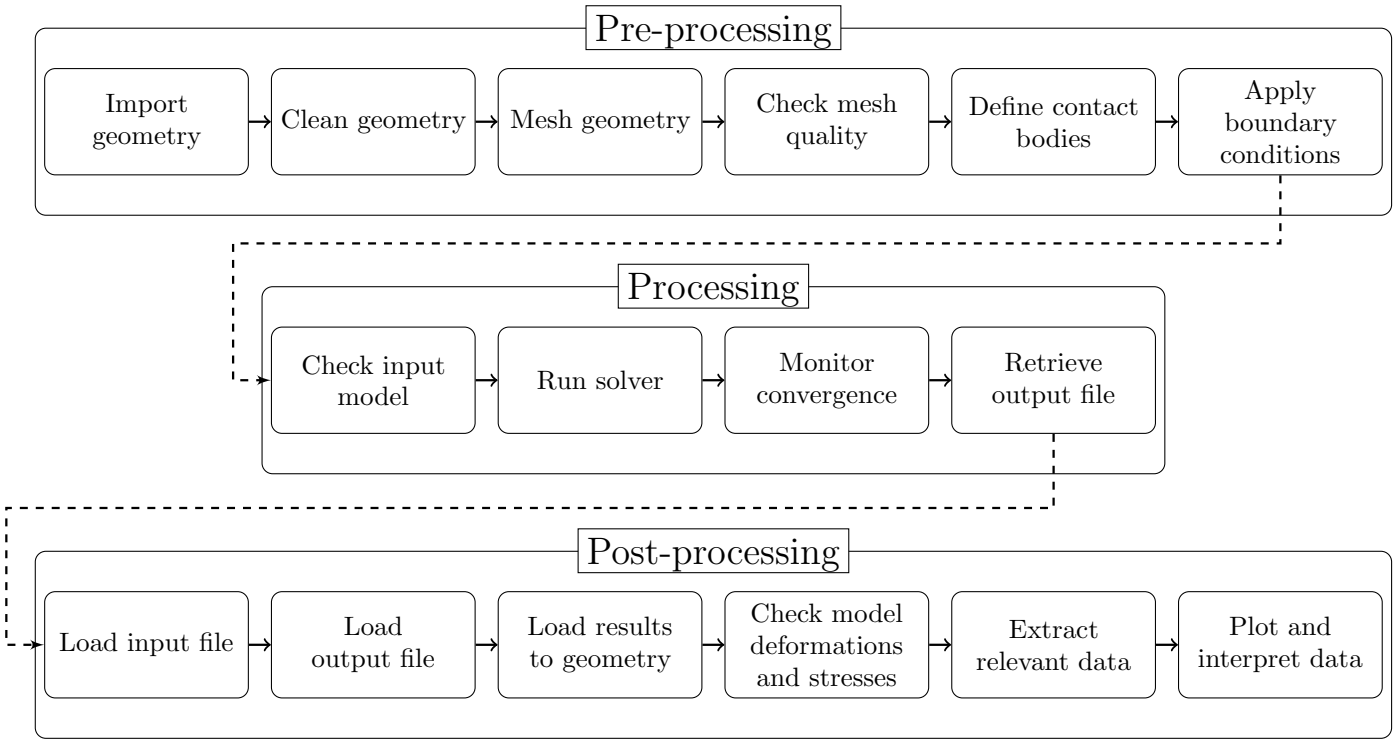

Figure 1.2: *Workflow for the FE simulations*

2 Theory

The aim of this thesis is to find a mathematical model of how the out-of-plane loading affects the slipping condition of a bolted joint based on the rigid body theory. In this chapter the concepts of slip and joint failure will be presented as well as some of the modelling techniques for bolted joints in FE analysis.

2.1 Failure Criteria

The joint will be considered failed when there is slip in the whole joint, meaning that the whole bolt area is slipping. This will ultimately initiate contact between the bolts and the bolt hole, creating a shear force on the bolt that the bolt is normally not designed to withstand.

2.2 Bolt Modelling

Modelling bolts in FE analyses has to be very carefully performed as the introduced boundary conditions can lead to behaviour that is far from accurate. Some ways to model bolts are presented in Table 2.1

Type	Pros	Cons
Beam Element Bolt	Computationally cheap	Does not capture separation
Solid Bolt	Captures head and nut behaviour Captures separation in contact	Computationally expensive
Threaded Bolt	Captures thread stresses If threads are completely modelled with rise it is possible to test torque to pre-tension	Extremely computationally expensive

Table 2.1: Different types of bolt modelling techniques

Some illustrations of the different modelling techniques available are displayed in Figure 2.1. The computationally cheapest way to model bolts are only good for very simple analyses where the actual slip condition is not of great importance. Since the bolt head is not there to apply another slip plane the, slip condition is greatly changed. Instead the bolt resists slipping motion with its full flexural stiffness. Meanwhile the threaded bolt technique is mainly good when thread specific behaviour needs to be analysed. The solid bolt modelling captures the stresses in the bolt body and the friction between the bolt head and the clamped part.

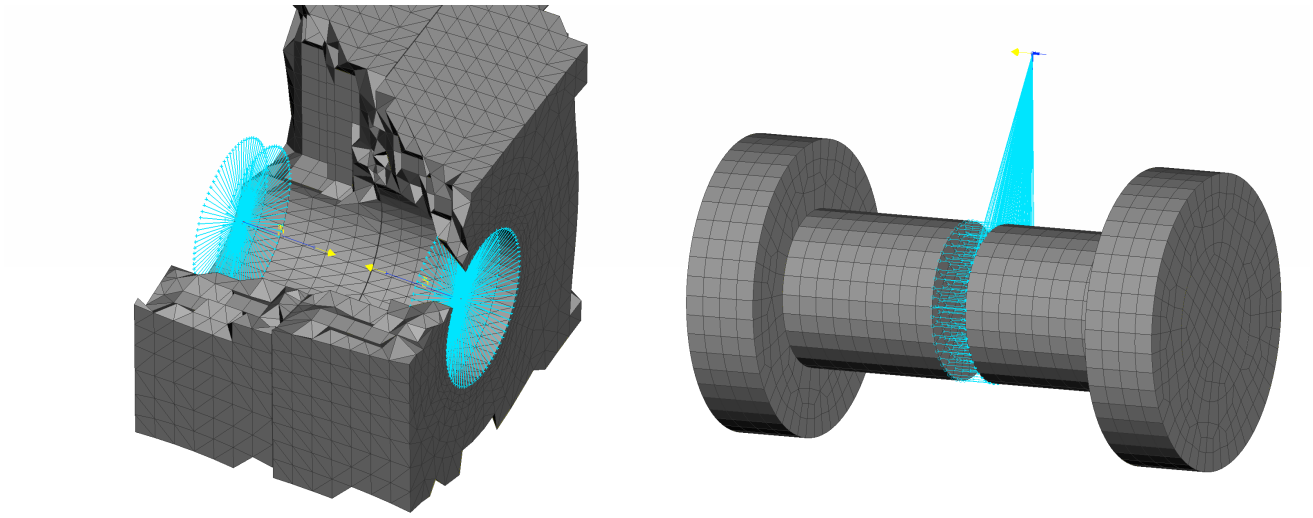

(a) *Rigid body elements on the inside of the holes connected with beam elements*

(b) *Multi-point constraint introduced after bolt is split*

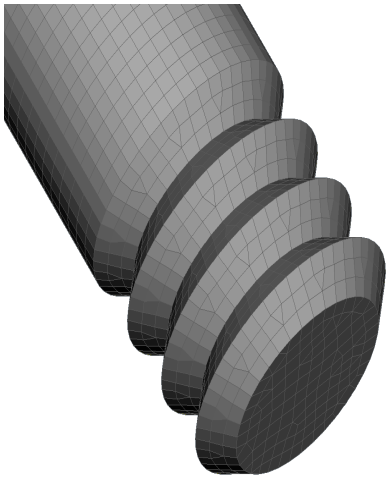

(c) *Threaded bolt*

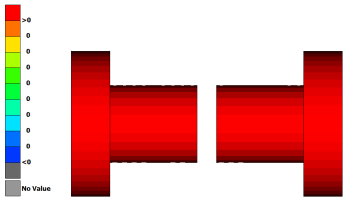

(d) *Bolt split and nodes tied with multi-point constraint*

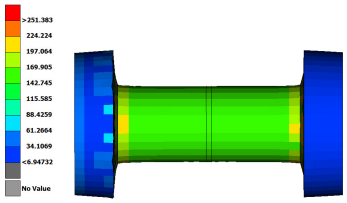

(e) *Bolt pre-stressed*

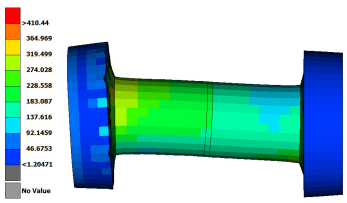

(f) *Bolt in loading just before slip*

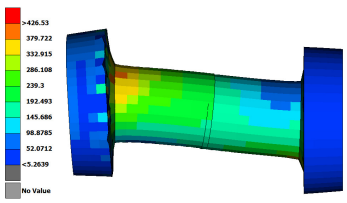

(g) *Bolt post slip*

Figure 2.1: *Stresses and displacements for different bolt models in various situations, deformation scale factor of 100*

During this thesis the solid bolt modelling technique will be used as this is a good approach for bolted joint analysis where the general bolt and joint behaviour is the target of the simulation.

2.3 Slip Condition

The slip condition for any point in a contact surface can be simplified to the clamping pressure multiplied by the friction coefficient. According to the Coulomb friction model, this is the maximum shear stress the point on the surface can resist before slip occurs. In Figure 2.2 the slip condition of a transversely loaded strip is shown. F_{cs} is the maximum friction force in the clamped plane and F_{bs} is the maximum friction force in the bolt head plane.

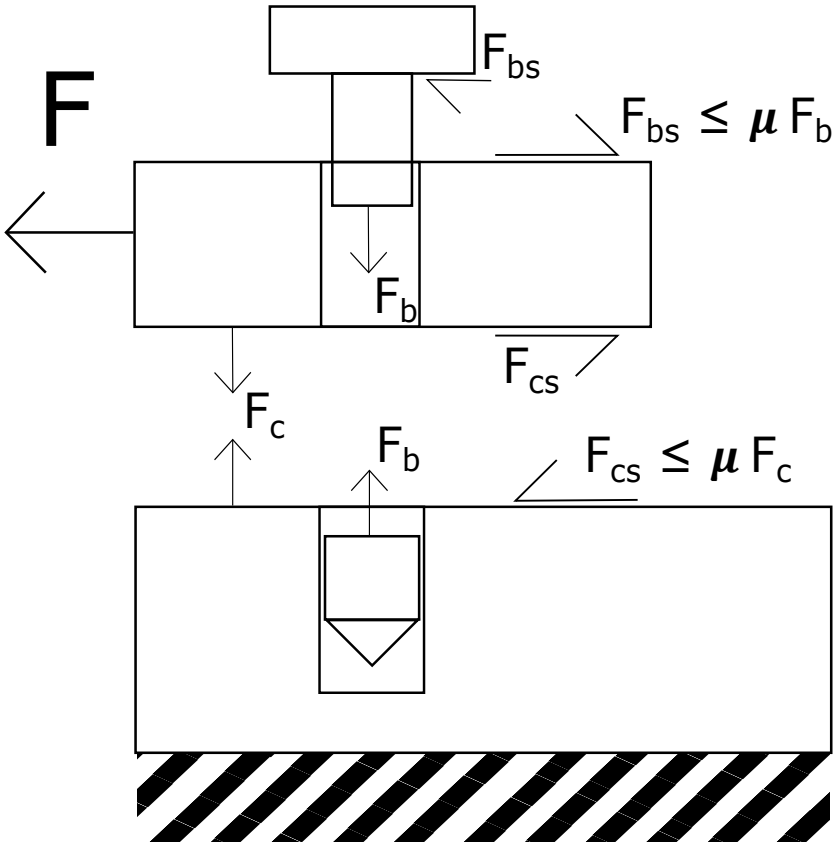

Figure 2.2: *Bolt area simplified as a strip with two slip planes*

From this figure the maximum friction force F_s and maximum allowed transverse load F to fulfil static conditions for the strip is:

$$F \leq F_s \leq \mu F_c + \mu F_b \tag{2.1}$$

If the strip is loaded in the axial direction of the bolt, a difference in F_b and F_c can be shown using force equilibrium, this will be treated further ahead in Section 2.4. It is also assumed that the bolt can carry the full slipping load before deflection.

2.4 Rigid Body Motion

Assuming rigid body theory, the effect of the out-of-plane load on the clamped areas can be derived by splitting it into two moments and one transverse force. First the out-of-plane force is derived by assuming rigid body motion around an axis through the centre of the plate. The superposition principle is then implemented on the two different load cases in the plane, one with the moment in the plane of the plate and one with the transverse forces, to obtain the final shearing force on the clamped area coming from the plate. The plate is considered rigid and the bolts are considered as elastic springs.

2.4.1 Joint Forces

Due to the applied external load, reaction forces in the clamping areas must be accounted for. Using rigid body theory, an expression for these forces depending on the applied load can be derived.

2.4.2 Out-of-Plane Moment

The out-of-plane moment will influence the clamping force of the separate bolt areas. To find this influence, an assumption that the moment will be distributed as a force on all bolts depending on the area of inertia is made. In Figure 2.3 the expected reaction forces can be seen.

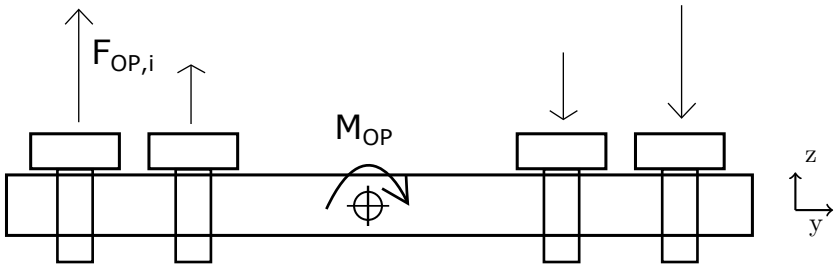

Figure 2.3: *Out-of-plane moment effect on the bolts*

Say that i is the bolt index and n is the number of bolts. The area moment of inertia around the centre of mass, $I_{par,x}$, using the parallel axis theorem [4] (see Appendix B.1), is then computed as:

$$I_{par,x} = \sum_{i=1}^{n} A_i \cdot y_i^2 \tag{2.2}$$

where A_i is the bolt cross section area and y is the y-coordinate of the bolt centre. The average pressure $P_{avg,i}$ in the bolts can then be calculated as (c.f. Appendix B.1):

$$P_{avg,i} = \frac{-M_{OP} \cdot y_i}{I_{par,x}} \tag{2.3}$$

where M_{OP} is the moment out of the plane induced by the applied load. Multiplying with the bolt cross sectional area yields the bolt axial force $F_{OP,i}$ created from the moment:

$$F_{OP,i} = P_{avg,i} \cdot A_i = \frac{-A_i \cdot M_{OP} \cdot y_i}{I_{par,x}} = \frac{-A_i \cdot M_{OP} \cdot y_i}{\sum_{j=1}^{n} A_j \cdot y_j^2} \tag{2.4}$$

An expression for the axial force induced by the out-of-plane moment, assuming that all bolt cross sections are

uniform, can then be calculated as:

$$F_{OP,i} = \frac{-M_{OP} \cdot y_i}{\sum_{j=1}^{n} y_j^2} \tag{2.5}$$

2.4.3 In-Plane Moment

The same procedure used in Section 2.4.2 can be used for the in-plane moment and an expression for the shearing force from the in-plane moment achieved. Figure 2.4 describes the reaction forces in the bolts from the in-plane moment and transverse force. Here r_i is the radial distance from the assumed centre of rotation and α_i the angle of F_{IP} to the x-axis.

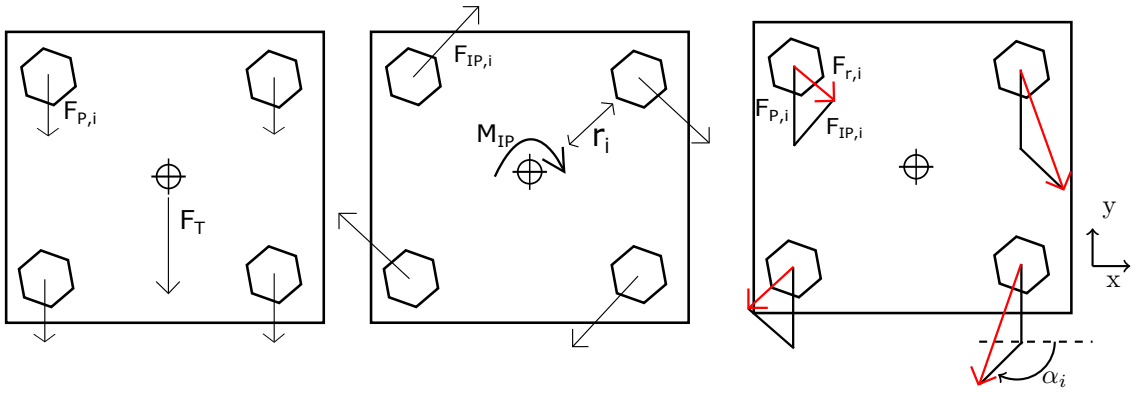

(a) *Transverse forces* (b) *In-plane moment* (c) *Resultant forces*

Figure 2.4: *Equilibrium for applied force and moment in centre of gravity for bolts*

The expression for the shearing forces $F_{IP,i}$ from the in-plane moment, M_{IP}, is computed using area moment of inertia, assuming uniform bolt cross section areas (see Appendix B.2 for further information):

$$F_{IP,i} = \frac{-M_{IP} \cdot r_i}{\sum_{j=1}^{n} r_j^2} \tag{2.6}$$

where r_i is dependent on the bolt coordinates x_i and y_i as:

$$r_i = \sqrt{x_i^2 + y_i^2}$$

2.4.4 In-Plane Force

The transverse force is then moved into the plane due to the moments introduced and is assumed to be divided equally as $F_{P,i}$ between the bolts:

$$F_{P,i} = F_T/n \tag{2.7}$$

where F_T is the applied load moved into the plane.

2.4.5 Resulting Forces

A vector sum is used to determine the resulting force $F_{r,i}$ acting on the clamped area in the plane. The angle α_i is given by:

$$\alpha_i = \begin{cases} \frac{\pi}{2} - \arctan\frac{y_i}{x_i} & \text{for } x \geq 0,\ y > 0 \\ \frac{\pi}{2} + \arctan\frac{|y_i|}{x_i} & \text{for } x > 0,\ y \leq 0 \\ \frac{3\pi}{2} - \arctan\frac{y_i}{x_i} & \text{for } x < 0,\ y < 0 \\ \frac{3\pi}{2} - \arctan\frac{|y_i|}{x_i} & \text{else} \end{cases}$$

The magnitude of the in-plane force is:

$$F_{r,i} = \sqrt{\left(\frac{M_{IP} \cdot r_i}{\sum_{j=1}^{n} r_j^2}\cos(\alpha_i)\right)^2 + \left(\frac{F_{P,i}}{n} + \frac{M_{IP} \cdot r_i}{\sum_{j=1}^{n} r_j^2}\sin(\alpha_i)\right)^2} \tag{2.8}$$

The clamping force $F_{c,i}$ can then be expressed as the preload force summed with the axial force from the out-of-plane moment:

$$F_{c,i} = F_{pre,i} - \frac{M_{OP} \cdot y_i}{\sum_{j=1}^{n} y_j^2} \tag{2.9}$$

The slip resistance $R_{slip,i}$ for any bolted area can then be expressed as:

$$R_{slip,i} = F_{c,i} \cdot \mu + F_{b,i} \cdot \mu \tag{2.10}$$

While the bolt retains its pre-load force F_{pre} since the plates are considered rigid, no deformation occurs in the bolt until separation, leading to:

$$F_{c,i} = F_{pre,i} + F_{OP,i} \tag{2.11}$$

$$F_{b,i} = F_{pre,i} \tag{2.12}$$

2.5 Worst Bolt Model

An expression for expected shearing forces and slip resistance in any bolt is now formulated. It can then be stated that the safety factor, s_{fac}, for any bolt is:

$$s_{fac,i} = \frac{R_{slip,i}}{F_{r,i}} \tag{2.13}$$

Eq. (2.13) is expanded, arriving at a formula for the safety factor against slip regarding local shear forces, meaning that this is not a safety factor for applied force but for the shear forces in the clamping areas.

$$s_{fac,i} = \frac{\left(2F_{pre,i} - \frac{M_{OP} \cdot y_i}{\sum_{j=1}^{n} r_j^2}\right) \cdot \mu}{\sqrt{\left(\frac{M_{IP} \cdot r_i}{\sum_{j=1}^{n} r_j^2}\cos(\alpha_i)\right)^2 + \left(\frac{F_P}{n} + \frac{M_{IP} \cdot r_i}{\sum_{j=1}^{n} r_j^2}\sin(\alpha_i)\right)^2}} \tag{2.14}$$

2.6 Total Joint Slip

Here Kulak's instant centre of rotation theory [5] is introduced, a model of when a joint experiences complete slip. Kulak's method assumes that the joint will slip in all bolts simultaneously and that it is possible to find a point around which the whole joint will rotate at the moment of slip. The critical load is then resolved by finding this point using moment equilibrium. In Figure 2.5 the loading direction and eccentricity e of the applied load P can be seen. This will be used to find the instant centre of rotation (I.C.), coordinate using moment equilibrium. This point must be on a line perpendicular to the load direction according to Eq. (2.16), passing through the intersection of the balance lines of the slip resistance of the clamped areas. So a balance line, shown with dashed line in Figure 2.5, is found by weighting the coordinates of the bolts with their slip resistance and finding their balance lines in both y-direction and x-direction.

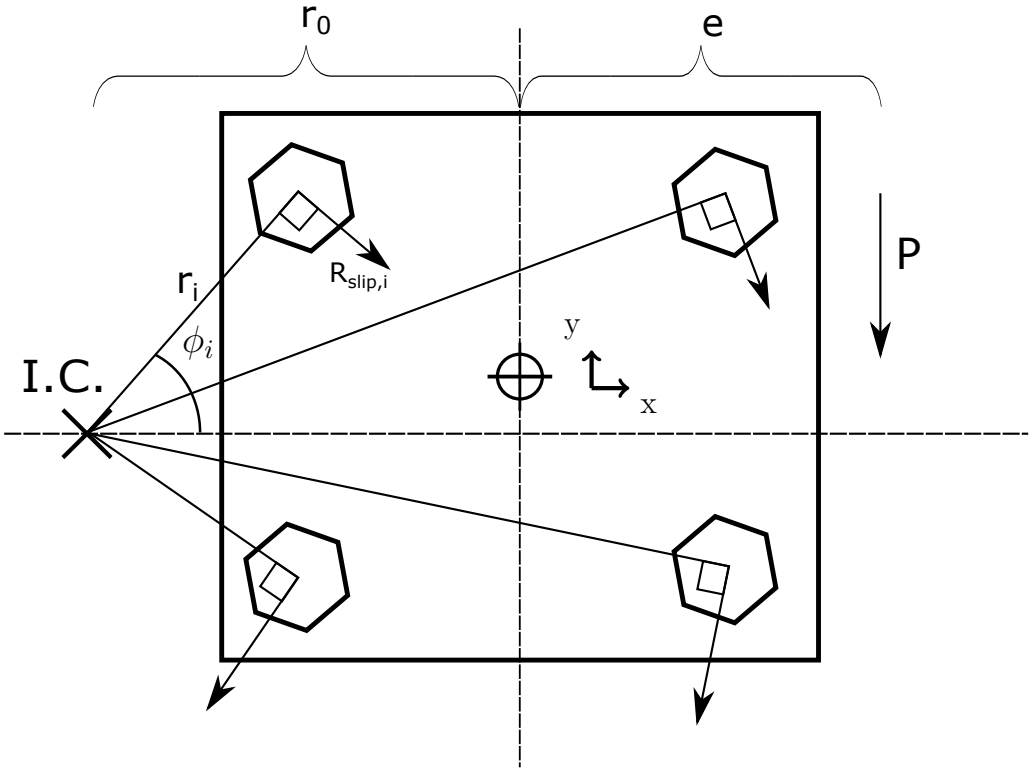

Figure 2.5: *Diagram of forces for moment equilibrium*

where r_0 is the distance from the intersection of the balance lines. The equilibrium equations can thus, according to Kulak [5], be stated as:

$$\uparrow: \quad \sum_{i=1}^{n} R_s \ \cos(\phi_i) - P = 0 \tag{2.15}$$

$$\rightarrow: \quad \sum_{i=1}^{n} R_s \ \sin(\phi_i) = 0 \tag{2.16}$$

$$\curvearrowright: \quad P(r_0 + e) - \sum_{i=1}^{n} R_s \ r_i = 0 \tag{2.17}$$

Here, Kulak's slip resistance term R_s is:

$$R_s = mk_sT_i \tag{2.18}$$

where m is the number of faying surfaces (slip planes), k_s is the friction coefficient of the surfaces and T_i is the clamping force. Kulak's theory can be extended to the case of varying slip resistance in the bolts. Assuming two slip planes between the plates and bolt heads, Kulak's slip resistance will be replaced by the slip resistance in the rigid body model, where the slip resistance is:

$$R_{slip,i} = (F_{b,i} + F_{c,i}) \cdot \mu \tag{2.19}$$

where F_b is the bolt force and F_c the clamping force. This slip resistance is valid assuming that both planes have the same friction coefficient and the bolts carry the full slip load before deflection. Introducing this new slip resistance gives a slip resistance that is individual to each clamped area. A new balance line must therefore be defined using the new slip resistances as weights placed on the bolt locations. These new balance lines, are defined in the x- and y-direction.

Using equilibrium for the system where the forces on the bolts are chosen to be the slip resistance $R_{slip,i}$, acting perpendicular to the I.C., describes the state right before slip. Here, it is possible to solve for the critical load P by iterating the point r_0.

$$\begin{aligned} P_1 &= \sum_{i=1}^{n} R_{slip,i} \cdot \cos(\phi_i) \\ P_2 &= \frac{\sum_{i=1}^{n} R_{slip,i} \cdot r_i}{(r_0 + e)} \end{aligned} \tag{2.20}$$

When $|P_1 - P_2| \leq tol$ the iterating is terminated and the critical load is determined by the equilibrium equations.

It is important to note that as the eccentricity of the load is approaching zero, i.e. the intersection of the balance lines, the equations (2.20) will be approaching the transverse slip resistance as can be seen in Figure 2.6a, meaning that no rotation will occur and the instant centre of rotation will be infinitely far away. Figure 2.6b illustrates this singularity as the eccentricity approaches zero.

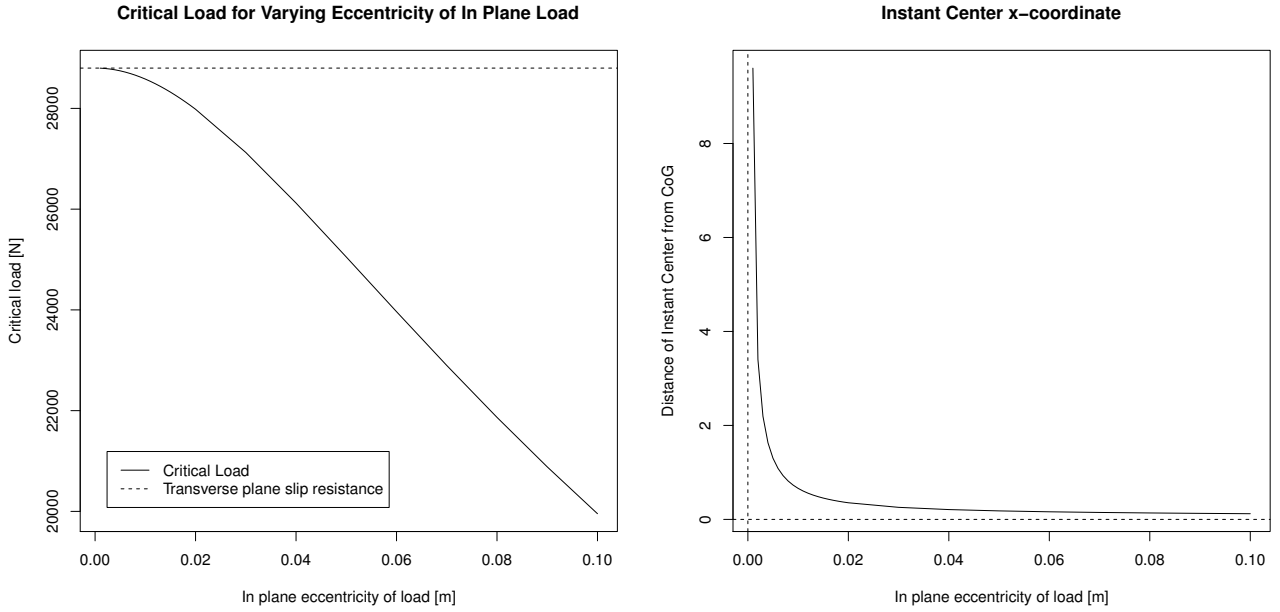

(a) *Critical load with varying eccentricity*

(b) *Distance of instant centre of rotation from balance line intersection*

Figure 2.6: *Singular and asymptotic behaviour of the instant centre of rotation method*

2.7 Elastic Members

The forces from the rigid body theories can be applied to the assumptions that the plates and bolts are elastic only in the clamping areas and rigid elsewhere. Using an expression for the material stiffness developed herein, a relationship between the external axial forces, the bolt forces and clamping forces are developed.

2.7.1 Clamping Force

A clamped area can be described as a system of springs in parallel where the material(s) being clamped is in series. To solve the equilibrium in this system the stiffness of the material is idealised as springs. It is assumed that all material experiencing deformation contributes to the stiffness only in the clamping direction. The material in the clamped areas can be assumed to deform in the shape of a frustum, as shown in Figure 2.7a, with a 30° angle, θ, according to Shigley [6]. Figure 2.7b shows a schematic representation of the spring system, where K_B is the bolt stiffness, K_{c1} and K_{c2} is the material stiffness, r_0 is the hole radius, r_1 is the bolt head radius and r_2 is the radius at depth x.

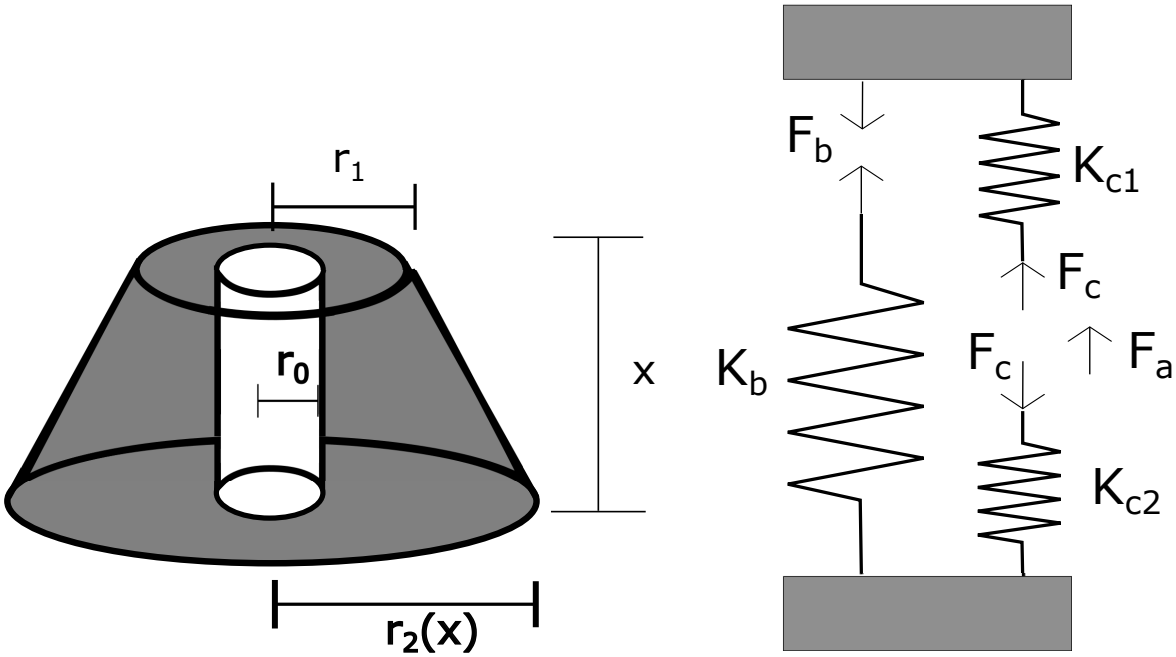

(a) *Deformation cone* (b) *Spring system of clamped area*

Figure 2.7: *Deformation cone and schematic of spring system for clamping area*

The axial deformation δ of a cross section A is used to find the stiffness of the frustum:

$$d\delta = \frac{Pdx}{EA} \tag{2.21}$$

where E is the Young's modulus of the material and P is the applied load. In the frustum a varying cross-sectional area along the axial direction is expressed as:

$$\begin{aligned} A &= \pi\left(r_2^2 - r_0^2\right) = [r_2 = r_1 + x \cdot \tan(\theta)] = \\ &= \pi\left(x\ \tan\theta + r_1 + r_0\right)\left(x\ \tan\theta + r_1 - r_0\right) \end{aligned} \tag{2.22}$$

The equation Eq. (2.21) can now be formed as the integral:

$$\delta = \frac{P}{\pi E}\int_0^L \frac{1}{\left(x\ \tan\theta + r_1 + r_0\right)\left(x\ \tan\theta + r_1 - r_0\right)}dx \tag{2.23}$$

Integrating Eq. (2.23) according to Mathematics Handbook [7] pg.156 Eq.49 yields the equation for elongation:

$$\delta = \frac{P}{\pi E 2 r_0 \tan\theta}\ln\frac{\left(L\tan\theta + r_1 - r_0\right)\left(r_1 + r_0\right)}{\left(L\tan\theta + r_1 + r_0\right)\left(r_1 - r_0\right)} \tag{2.24}$$

The equation for stiffness is:

$$k = \frac{P}{\delta} \tag{2.25}$$

The final stiffness K_c for the clamped material thus becomes:

$$K_c = \frac{\pi E 2 r_0 \tan\theta}{\ln\dfrac{\left(L\tan\theta + r_1 - r_0\right)\left(r_1 + r_0\right)}{\left(L\tan\theta + r_1 + r_0\right)\left(r_1 - r_0\right)}} \tag{2.26}$$

This expression is only valid as long as the assumption of the strain cone angle not varying through the thickness is true. Very thick plates will have a more barrel shaped strain frustum [8].

With the stiffness K_c and the bolt stiffness K_b, the clamping area can be idealised as a spring system as illustrated in Figure 2.7b. The applied external force gives a new elongation of the system:

$$\Delta L = \frac{F_a}{K_b + \left(\frac{1}{K_{c1}} + \frac{1}{K_{c2}}\right)^{-1}} = \left\{ K_C = \left(\frac{1}{K_{c1}} + \frac{1}{K_{c2}}\right)^{-1} \right\} = \frac{F_a}{K_b + K_C} \tag{2.27}$$

Before the external load is applied $F_c = F_{pre}$, where F_{pre} is the pre-tension. Using the rigid body theory to get the applied force in all bolts, the updated clamping forces and forces in the bolts can be found:

$$F_c = F_{pre} - \Delta L \left(\frac{1}{K_{c1}} + \frac{1}{K_{c2}}\right)^{-1} = F_{pre} - \Delta L K_C \tag{2.28}$$

$$F_c = F_{pre} - \frac{F_a}{K_b + K_C} K_C = F_{pre} - \frac{F_a}{\frac{K_b}{K_C} + 1} \tag{2.29}$$

$$F_b = F_{pre} + \Delta L K_b = F_{pre} + \frac{F_a}{\frac{K_C}{K_b} + 1} \tag{2.30}$$

Clamping Diagram

The clamping forces can be described in a diagram as shown in Figure 2.8. Where F_a is the axial external force on the joint that leads to new deformations, Δd_b and Δd_c, in the joint as well as new clamping forces and bolt forces. ΔF_b and ΔF_c is the change of bolt and clamping force. If an axial load is applied on the joint, a reduction of the clamping force ΔF_c and increase of the bolt force ΔF_b is expected. Please refer to "Lärobok i Maskinelement" [9], for more in-depth explanations of clamping diagrams.

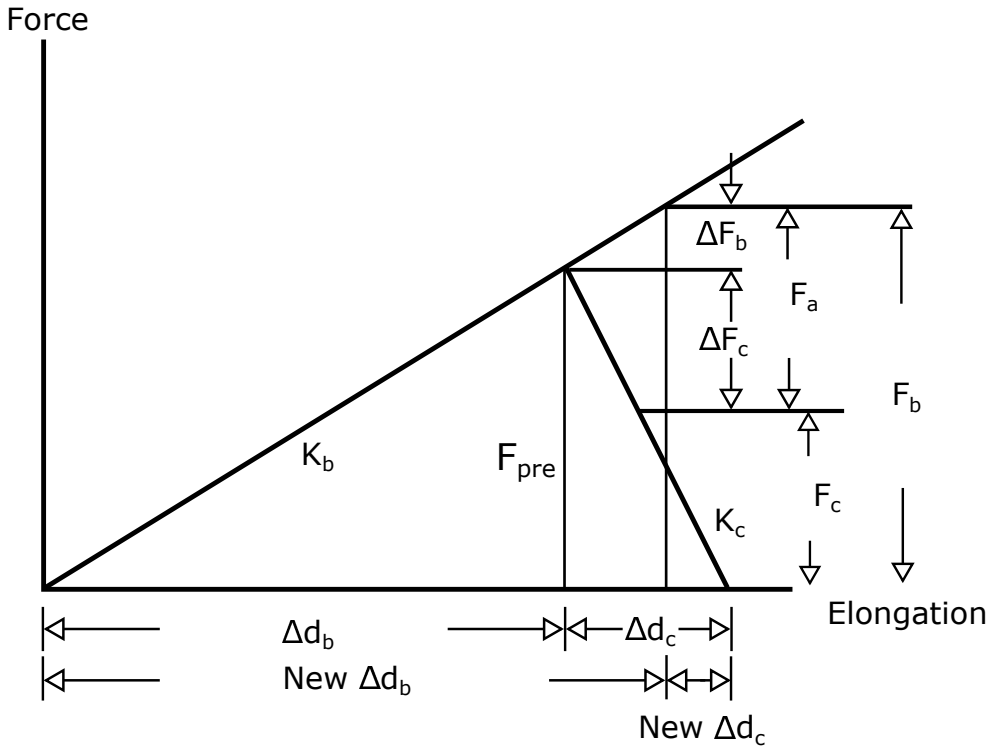

Figure 2.8: *Clamping Diagram*

2.7.2 Effect of Axial Forces on Slip Resistance

By introducing these new stiffnesses it is possible to formulate a net change in clamping forces due to the applied axial load. The bolt and clamped material both experience the preload force. The slip resistance without any axial load on the clamped area is then assumed to be:

$$R_{slip,i} = 2F_{pre}\mu \tag{2.31}$$

The new forces after introducing the elongation from the external force on the bolt and clamped material is calculated as:

$$\begin{aligned} F_b &= F_{pre} + \Delta L K_b \\ F_c &= F_{pre} - \Delta L K_C \end{aligned} \tag{2.32}$$

The new slip resistance is then:

$$R'_{slip,i} = (F_b + F_c)\,\mu \tag{2.33}$$

The change in slip resistance ΔR_{slip} is:

$$\Delta R_{slip} = R'_{slip} - R_{slip} = (F_b + F_c - 2F_{pre})\,\mu = \Delta L\,(K_b - K_C)\,\mu = F_{change}\mu \tag{2.34}$$

Therefore, the net change in clamping and bolt force F_{change}, defined in Eq. (2.34) is calculated as:

$$F_{change} = \Delta L\,(K_b - K_C) = \left\{\Delta L = \frac{F_a}{K_b + K_C}\right\} = \left(\frac{2K_b}{K_b + K_C} - 1\right) F_a \tag{2.35}$$

This means that the combined clamping forces decrease depending on the stiffness of the plate compared to the bolt. In the areas where the axial force is negative, meaning compressive for the clamping parts, there is a proportional increase in slip resistance according to the theory.

3 Finite Element Analysis

To validate the previously developed theory, an FE model was created and meshed in the program ANSA. The model was then solved using MSC's NASTRAN SOL400 with various choices of parameters. These results were used to compare the theoretically developed model against the behaviour simulated by the FE method.

3.1 Contact Pressure

In Figure 3.1 four plots of the contact normal pressure show some interesting patterns of the contact pressure and how it develops as the joint is loaded. The contact is separated around the hole of the bolts even before slip, which in a cyclic loading scenario could lead to fretting wear.

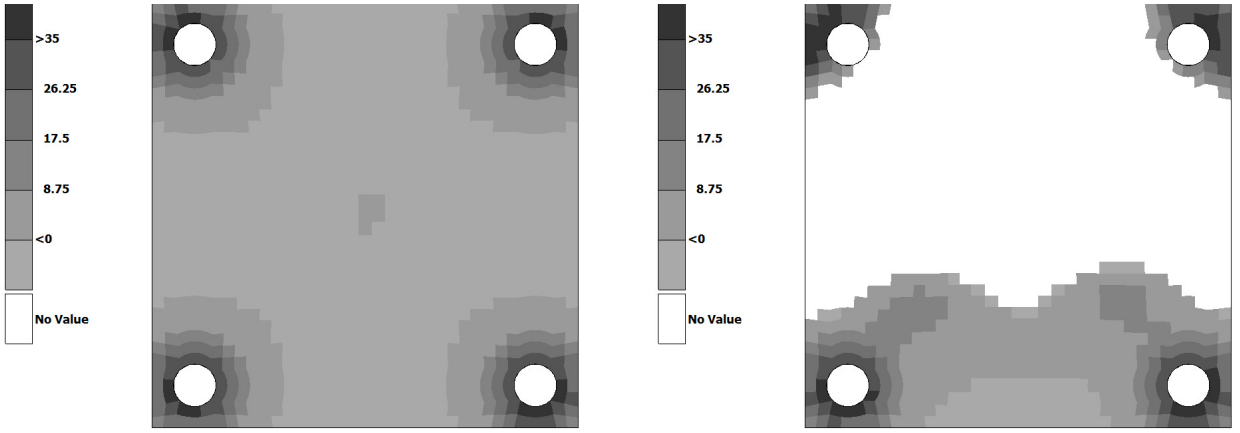

(a) *Contact normal pressure after preload step*

(b) *Contact normal pressure at 25% load application*

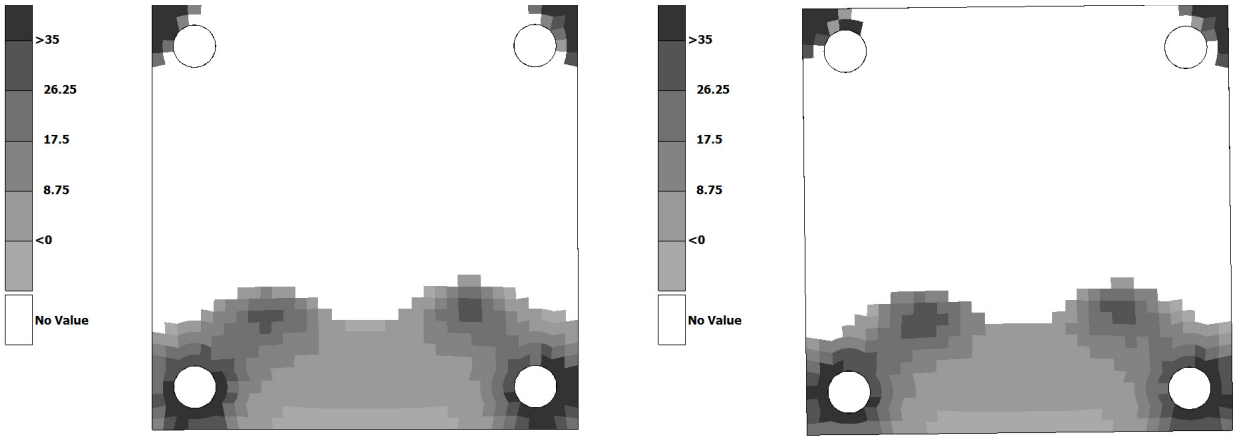

(c) *Contact normal pressure just before slip*

(d) *Contact normal pressure just after slip*

Figure 3.1: *Contact normal pressure of plate experiencing out-of-plane load*

The effects of the out-of-plane load can be seen in Figure 3.2 where the deformation is scaled by a factor of one hundred. The geometrical effects of the out-of-plane load, which could be one of the explanations of the increased slip resistance, is clearly shown.

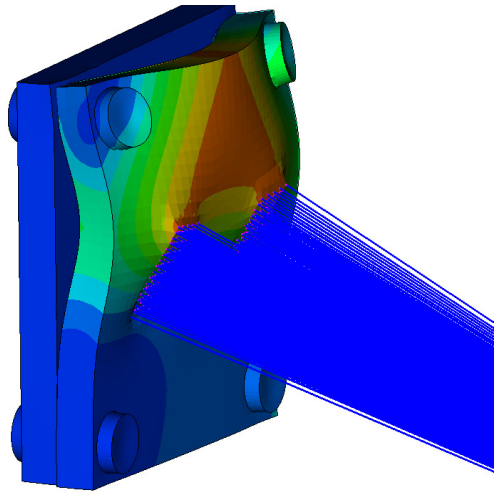

Figure 3.2: *Deformation with scale factor of 100*

3.2 Slip Detection

Using a nonlinear quasi-static solver means that iterations during contact sliding will be made until equilibrium is reached. Slip is thus detected by the solver and can be output as contact status, where the gap function can be open or closed, and the contact in sliding or sticking. Sliding here means that the contact has been in sliding condition during the iteration, since the solver reaches equilibrium during static conditions the contact cannot be in actual sliding during any finished load step. This can lead to convergence issues if the sliding motion is not constrained. For example, a block sliding on a slope is not constrained and the equilibrium condition for the sliding block is not reachable by the solver unless the block is constrained by a spring or similar, thus decreasing contact shear force the further it slides.

Slip can be described as a plastic event. The movement is non-conservative and cannot be reversed by deloading, detecting global slip can therefore be done by observing the displacement of say the loading point. When this points displacement starts behaving plastically it can be assumed that the joint is slipping.

3.3 Critical Loads

Critical loads are picked by hand from the curves using the assumption that total slip in the joint is reached when the stiffness is heavily reduced. The critical load is then said to be the one that is at the onset of slip or just before slip. The models are loaded using Rigid Body Elements (RBEs) connected to a node, placed off-centre in the plane and varied out-of-plane distance, taking a prescribed load.

3.3.1 Model 1

Figure 3.3a illustrates how the RBEs are connected to the model from the loadpoint. The loadpoint can then be varied in its position to investigate the difference of increased moment arm out of the plane. Figure 3.3b shows the critical slipping loads depending on the length out of the plane of the loadpoint.

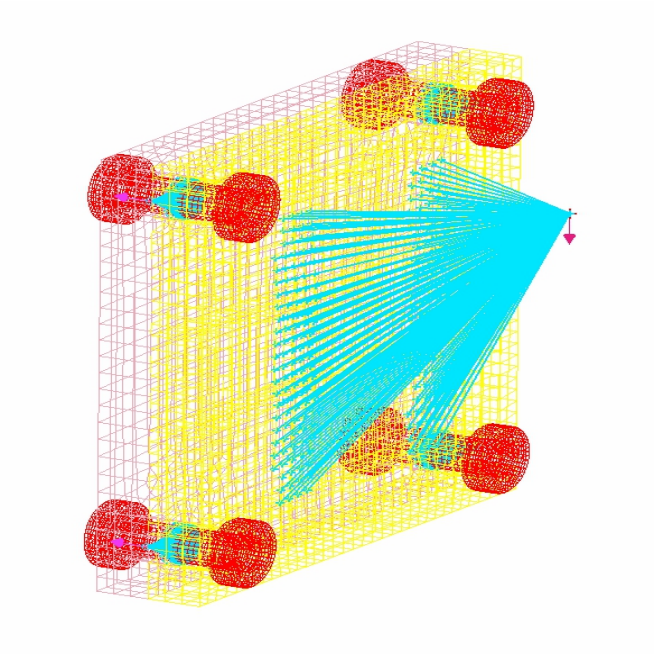

(a) *FE Model 1*

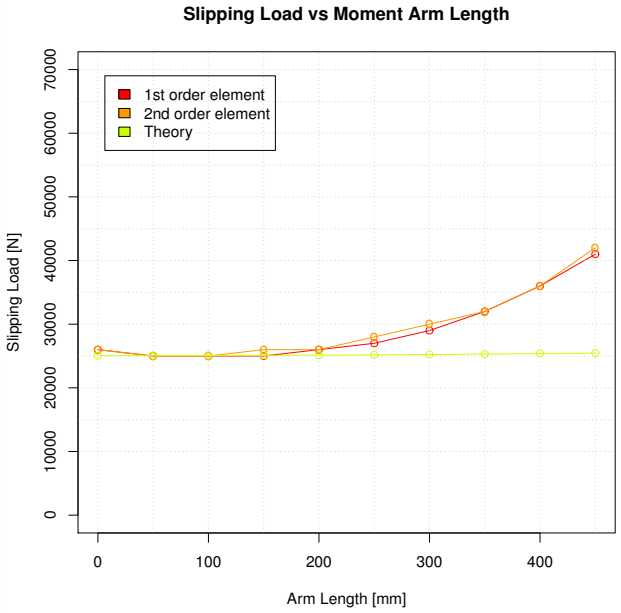

(b) *Slip determined by hand from load displacement curves*

Figure 3.3: *Discretised model and critical loads for model 1*

Figure 3.4 shows the displacements of the individual models for the loadpoint in the loading direction. It is possible to observe a sticking point halfway through the slip when modelling with the second order elements.

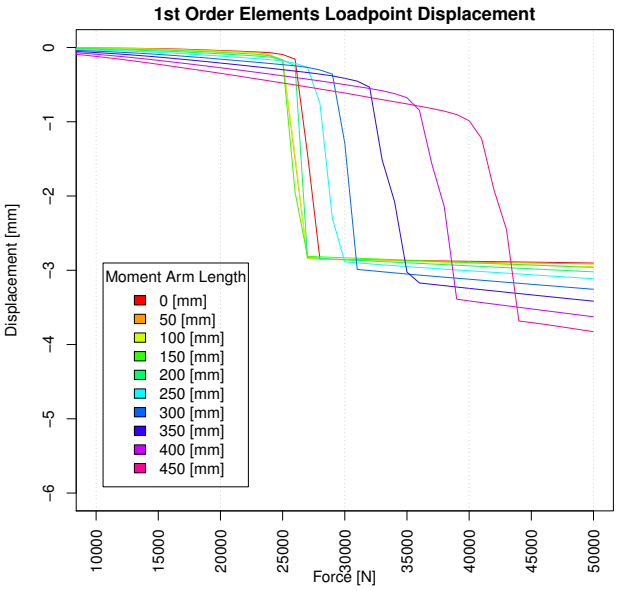

(a) *Displacement curve for first order elements*

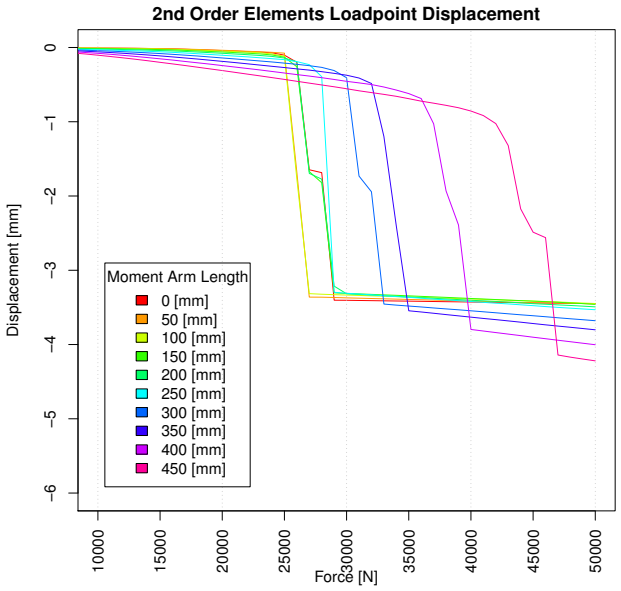

(b) *Displacement curve for second order elements*

Figure 3.4: *Displacements of the loadpoint for each load step of model 1*

3.3.2 Model 2

As can be seen from Figure 3.5a, Model 2 has a slightly smaller area of load application, decreasing the flexural stiffness of the plate and allowing for more geometrical distortion of the plate. From Figure 3.5b the critical loads can clearly be seen to increase compared to Model 1.

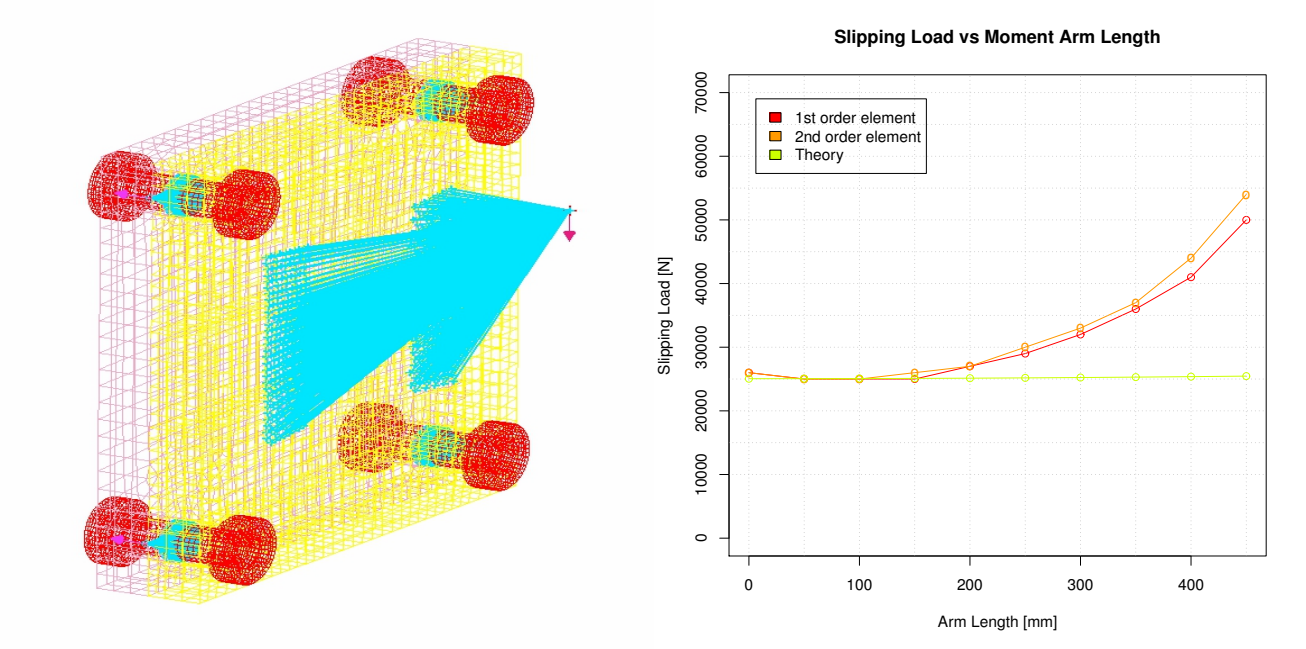

(a) *FE Model 2*

(b) *Slip determined by hand from load displacement curves*

Figure 3.5: *Discretised model and critical loads for model 2*

In Figure 3.6a the sticking halfway through sliding before the next slip to the bolts catching the plate can be seen in the first order element simulation.

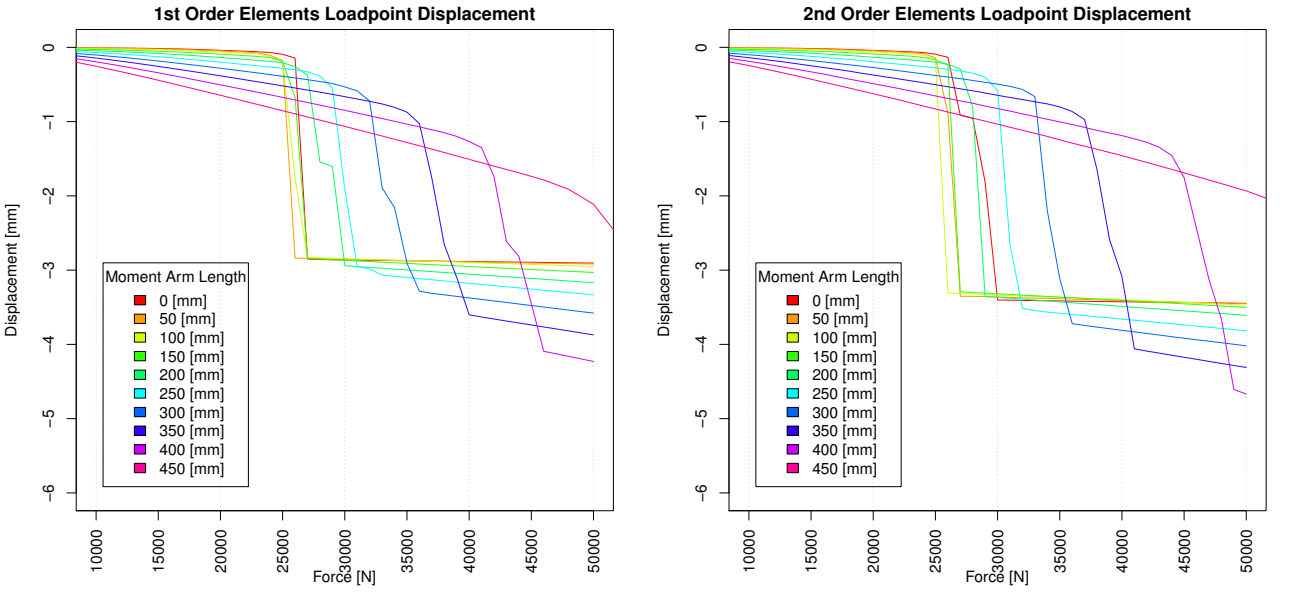

(a) *Displacement curve for first order elements*

(b) *Displacement curve for second order elements*

Figure 3.6: *Displacements of the loadpoint for each load step of model 2*

3.3.3 Model 3

Model 3 has the smallest area of load application. This further decreases the stiffness of the plate, leading to even larger geometrical distortions. The severe increase in slip resistance is reflected in the plot of the critical load Figure 3.7b. The increase in slip resistance is then assumed to be due to geometrical effects mostly.

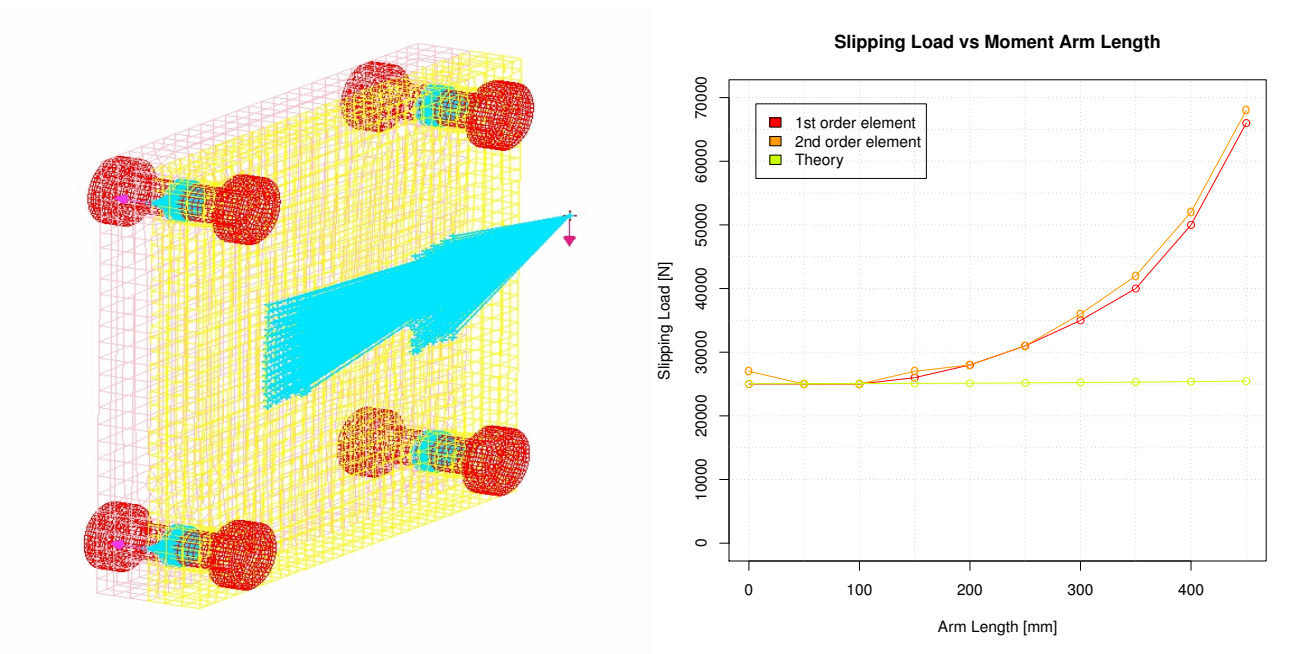

(a) *FE Model 3*

(b) *Slip determined by hand from load displacement curves*

Figure 3.7: *Discretised model and critical loads for model 3*

In Figure 3.8 the individual displacements are observed to have lowered stiffnesses due to the decreased flexural stiffness of the plate.

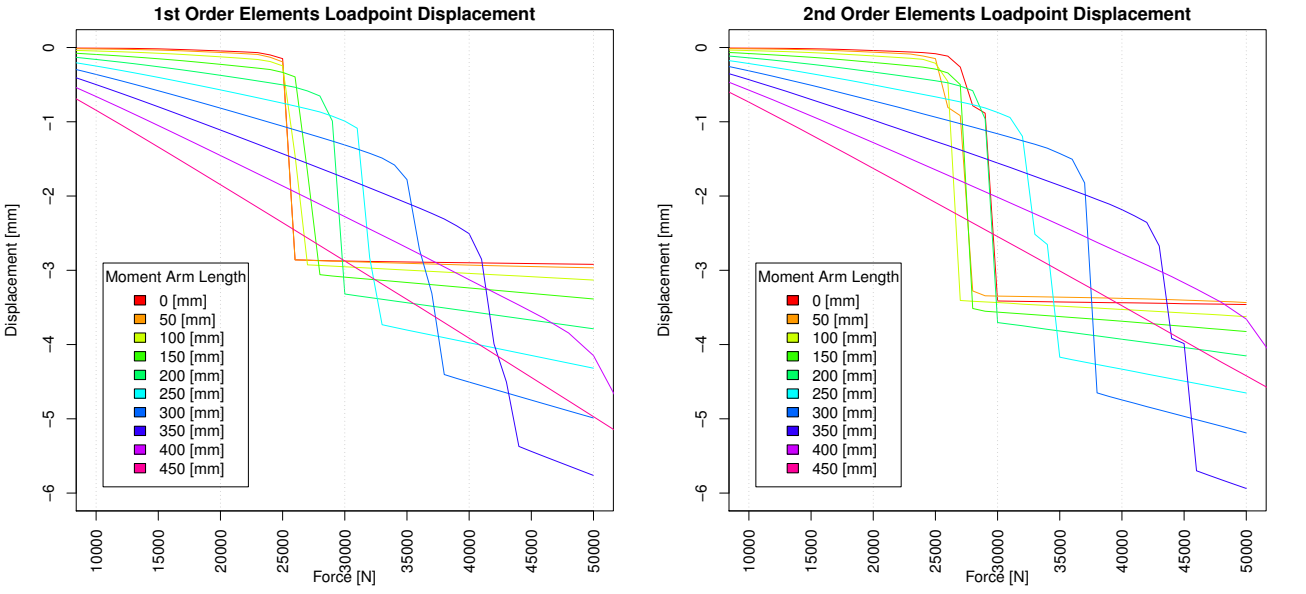

(a) *Displacement curve for first order elements*

(b) *Displacement curve for second order elements*

Figure 3.8: *Displacements of the loadpoint for each load step of model 3*

3.3.4 Small Displacements

With the large displacements formulation turned off, the results are still similar to large displacements. Figure 3.9b illustrates the similarities.

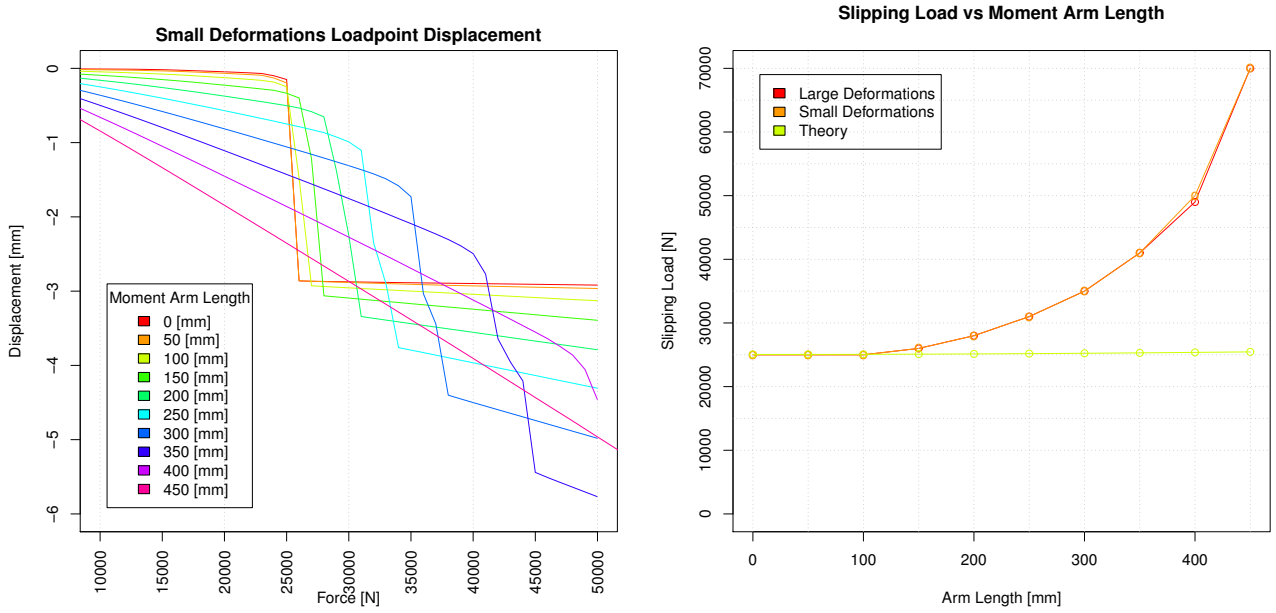

(a) *Displacement curve for first order elements* (b) *Displacement curve for second order elements*

Figure 3.9: *Displacements of the loadpoint for each load step and critical loads for model 3 with large displacement formulation and small displacement formulation*

3.3.5 Stiff Plates

The Young's modulus of the plate material was increased severely, making the plates rigid compared to the bolts, and the simulations were re-run. Figure 3.10b reveals that the assumption of rigid plates fits well with the rigid body theory developed.

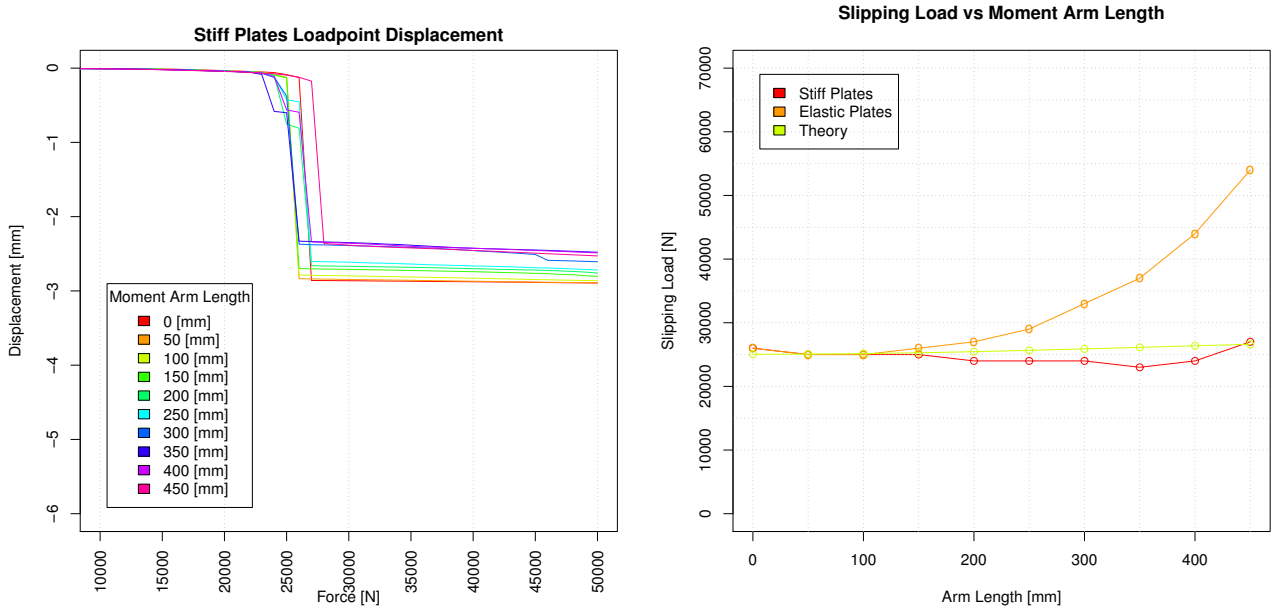

(a) *Displacement curve for first order elements* (b) *Displacement curve for second order elements*

Figure 3.10: *Displacements of the loadpoint for each load step and critical loads for model 2 with stiff and elastic plates*

3.3.6 Observations

From the FE results, a clear increase in the slip resistance of the joint with increasing moment arm can be seen. However it is also observed that the decrease in flexural stiffness also increases the slip resistance of the joint. This leads to the belief that the increasing slip resistance is a geometrical effect of the plate distortion. The model with stiff plates confirms that the plate shape has a big effect on the slip resistance.

3.4 Bolt Forces

The bolt forces during loading are extracted from the FE model. These can then be compared to the forces from the theoretical model and give a clue about how accurate the theory is in estimating the clamping forces in the bolted areas. Figure 3.11 shows the theoretical bolt forces for a certain load case compared to the FE bolt forces for that same load case.

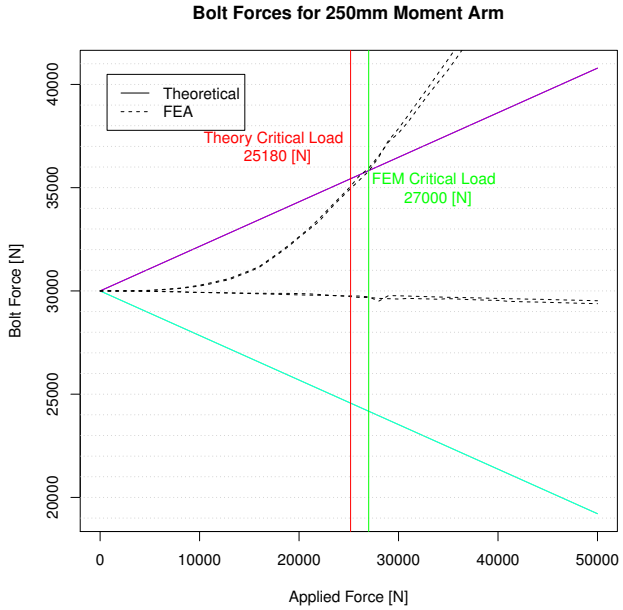

(a) *Bolt forces in joint with 250 [mm] moment arm*

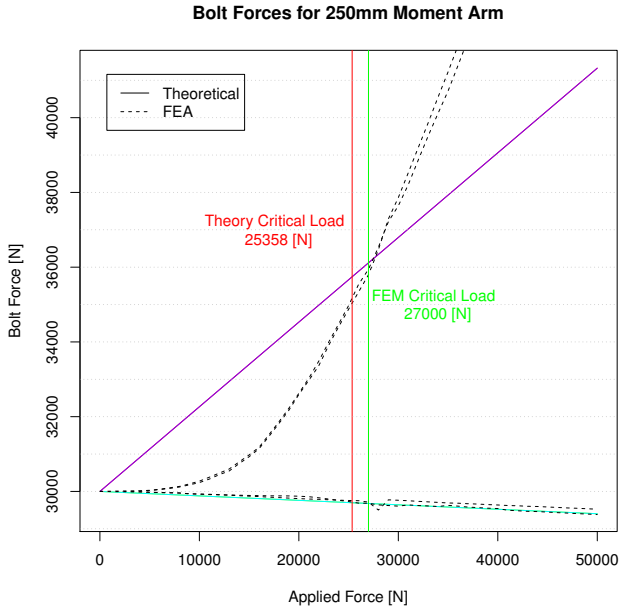

(b) *Bolt forces in joint with 250 [mm] moment arm with adjusted load point application to match lower bolt pair*

Figure 3.11: *Plot of bolt forces from FE simulations compared to the theoretical bolt forces during loading*

As can be seen in Figure 3.11a the theory predicts bolt forces in the compressive area that are much lower than the FE results. If the assumption of the plate rotating about the centre is changed to rotation closer to the bottom pair the compressive bolt pair forces can be matched more accurately by the theory, as seen in Figure 3.11b. The bolt forces in the FE simulations remain approximately unchanged in the compressive zone.

In Figure 3.12 the quadratic behaviour of the bolt forces with the increasing load arm coming from the FE analysis can be observed. The theory meanwhile shows completely linear development of the bolt forces with increasing moment arm.

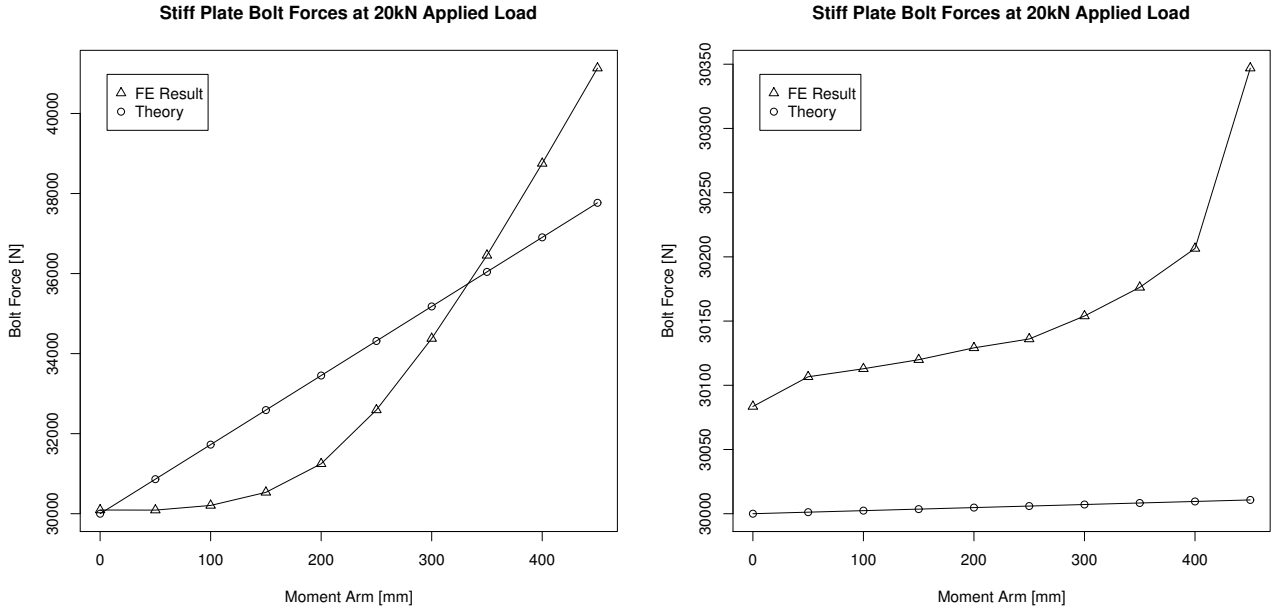

(a) *Bolt force in top right bolt at 20 kN applied load with varying moment arm on an elastic plate*

(b) *Bolt force in top right bolt at 20 kN applied load with varying moment arm on a stiff plate*

Figure 3.12: *Plot of bolt forces during loading*

A large increase in the bolt forces can be seen for the bolts in the tensile area going well beyond the predicted values of the theory. Due to the elasticity of the plate it can be observed that forces are not only taken in the bolted areas, this leads to the conclusion that the bolts in the compressive area will not experience the same compressive displacement as the opposite pair. The bolt forces can then be observed to be fairly constant in the compressive area of the joint. Meanwhile the clamped material still has to take up the increased compressive force, thus increasing the slip resistance in that area.

3.5 Real Model Simulation

Using a geometry provided by Ålö seen in Figure 1.1 and modified as in Figure 3.13, a simulation of the global slip resistance was made, this ended up providing further proof that the slip resistance of the joint is improved with increasing moment arm.

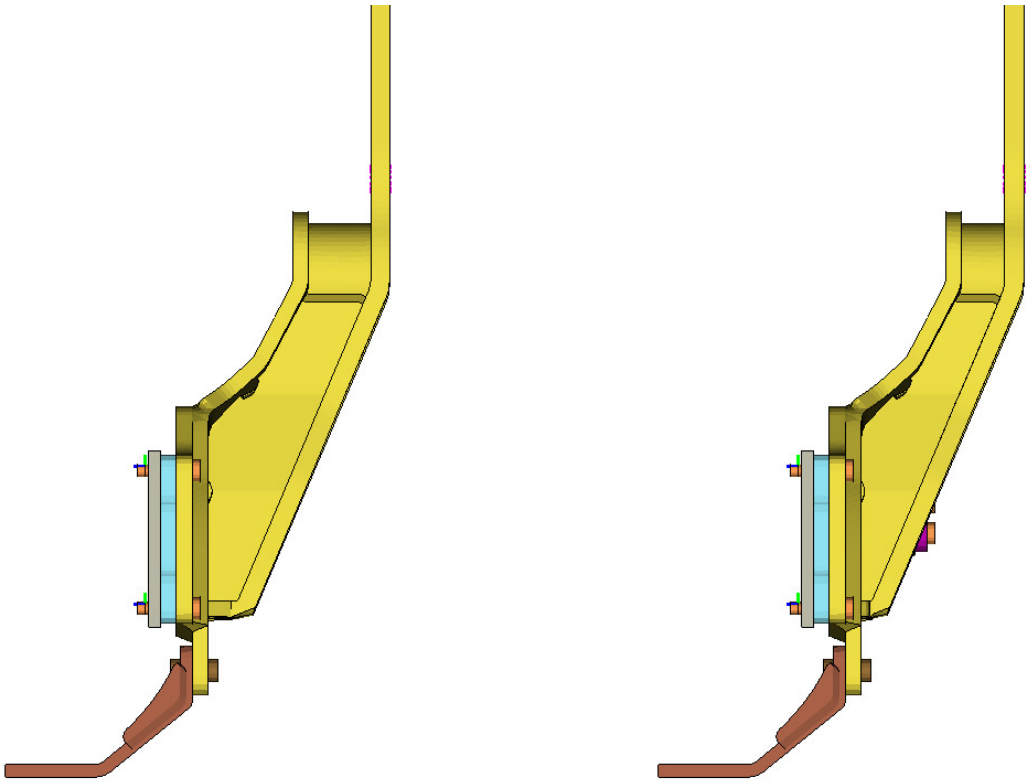

(a) *Model with greater out-of-plane moment arm* (b) *Model with shorter out-of-plane moment arm*

Figure 3.13: *Modified models*

In Figure 3.14 the slipping load is detected and can be observed to differ between the two models, where the model with increased out-of-plane moment arm has a small but visible increase in slip resistance. This is then compared to the theory developed, where the increase in slip resistance is observed to be insignificant compared to the simulations. These observations follow the patterns observed in the previous models.

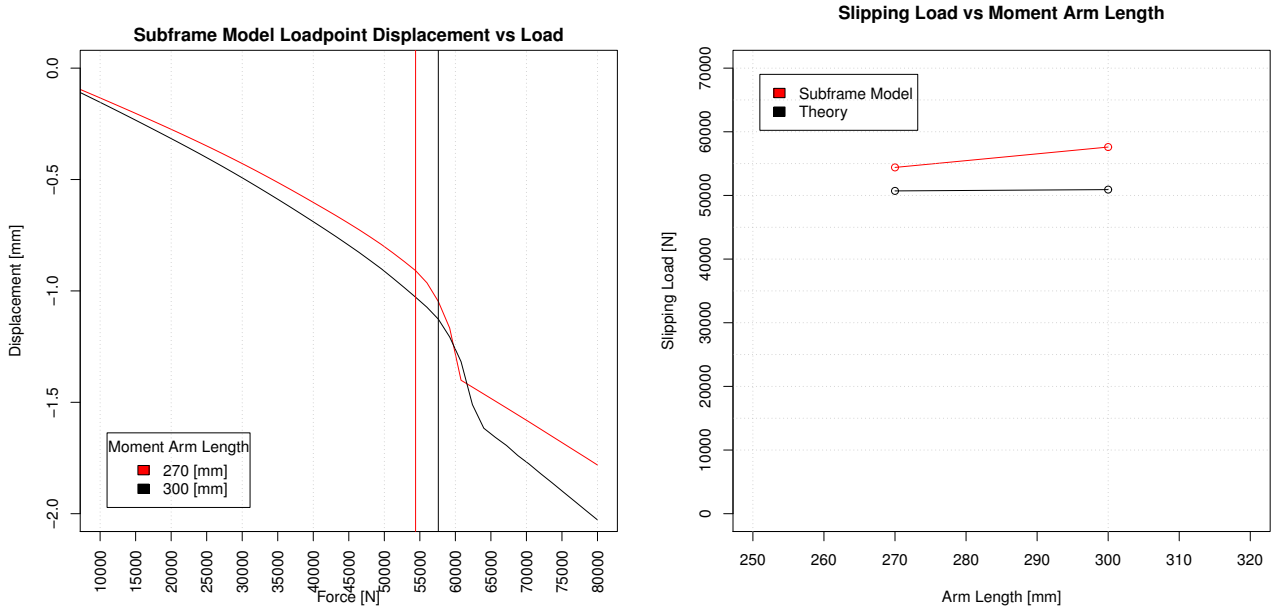

(a) *Displacement curve for subframe model* (b) *Comparison of theory to simulation*

Figure 3.14: *Displacements of the loadpoint for each load step of subframe model*

In Figure 3.15 the forces in the bolts obtained from the FE simulation is compared to the forces expected by the theory. The rigid body mode is correlated to match the bolts in the compressive zone, but again the theory fails to capture the extreme bolt forces on the tensile zones.

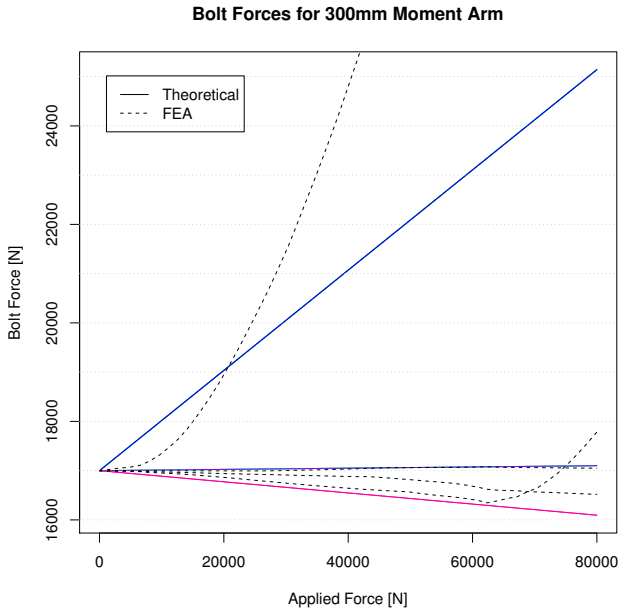

Figure 3.15: *Bolt forces from FE simulation compared to theory with correlated rigid body mode to match compressive bolts*

4 Discussion

Plastic Axial Loads

Initial experimentation in an FE environment suggests that the slip capacity of a joint increases as the moment arm out of the plane increases. However, it is not the author's recommendation to design against slip by moving the load further from the joint, as care must be taken so that the bolts do not enter the plastic zone as this could mean abrupt failure of the joint. The theory developed in this thesis can be used to predict bolt forces to foresee such plasticity, but unfortunately the bolt forces predicted in the theory does not correlate with the FE results.

Bolt Head Slip Resistance

The bolts in the theory developed in this thesis are assumed to carry the slipping load without deflecting. However, in a more accurate setting, this is not true. At the onset of transverse loading, the bolt can be modelled as a beam with a transverse load. This means that the bolt head force carrying condition is a mix of the slip condition and the flexural stiffness of the bolt as:

$$F_s \leq min \begin{cases} \mu F_b \\ \delta K_f \end{cases} \tag{4.1}$$

where δ is the deflection of the bolt head and K_f is the flexural stiffness of the bolt. This equation shows clearly that at the immediate onset of loading there is no contribution from the bolt head. The bolt does not contribute to any resistance of the slipping load until it has started to deflect.

Fatigue In Bolts

The introduced axial loads from the out-of-plane load could in a cyclic loading scenario lead to fatigue of the bolts, thus leading to joint failure. Using fatigue theory combined with the bolt forces or the maximum stress in the bolt calculated with Appendix B.1 Eq. (B.3) the number of cycles before failure could be calculated and that bolt can then be removed from the slip resistance calculation.

4.1 Future Work

- Further investigation of the geometrical shape effect on slip condition must be conducted.
- A more accurate method for finding the bolt loads theoretically must be developed as this can provide insight on how large effect the out-of-plane load has on the axial loads of the bolts.
- A fatigue analysis of the bolts should also be conducted as the cyclic axial loading is likely to result in fatigue.
- An investigation regarding the pre-tension loss from the cyclic axial loads should also be considered.
- An experimental study in a test rig should be conducted to validate the FE modelling.

References

[1] MSC Software. MSC Nastran 2014.1, Nonlinear User's Guide, SOL 400 (2014).
[2] M. Andreasson, MSC Software. MSC Nastran SOL400 Workshop (2016).
[3] MSC Software. MSC Nastran 2014.1 Documentation (2014).
[4] L. Råde and B. Westergren. *Handbok och formelsamling i Hållfasthetslära*. KTH, (2010).
[5] G. L. Kulak. Eccentrically Loaded Slip-Resistant Connections (2003).
[6] J. E. Shigley. *Mechanical Engineering Design*. McGraw-Hill Book Company, Inc, (1963).
[7] L. Råde and B. Westergren. *Mathematics Handbook for Science and Engineering*. Studentlitteratur, (2007). ISBN: 91-44-03109-2.
[8] K. H. Brown et al. Guideline for Bolted Joint Design and Analysis: Version 1.0 (2008).
[9] M. Mägi and K. Melkersson. *Lärobok i Maskinelement*. EcoDev International AB, (2006).
[10] R. Helfrich and I. Pflieger. Simulation and Optimization of Part Connections (2010).
[11] P. Wriggers. *Computational Contact Mechanics, Second Edition*. Springer, (2006). ISBN: 978-3-540-32608-3.
[12] M. Shillor, M. Sofonea and J. J. Telega. *Models and Analysis of Quasistatic Contact, Variational Methods*. Springer, (2004). ISBN: 978-3-540-44643-9.

Appendices

A Joint Designer Program

In this chapter the program developed to both compare the theory and FE results will be presented. The program developed can be used by, for example, a screw joint designer to find out how different bolt configurations and placement of load affect the critical load of the joint.

A.1 Interactive Script

The theory has been developed and is implemented as an interactive script/program, where the user can define:

- Bolt positions
- Bolt pre-tension
- Bolt and material Young's modulus
- Plate thickness and bolt dimensions
- Friction coefficient
- In-plane eccentricity and out-of-plane eccentricity of the load

In Figure A.1 the output from the script is shown, where the user will get data such as critical load, centre of rotation, and clamped area slip resistances.

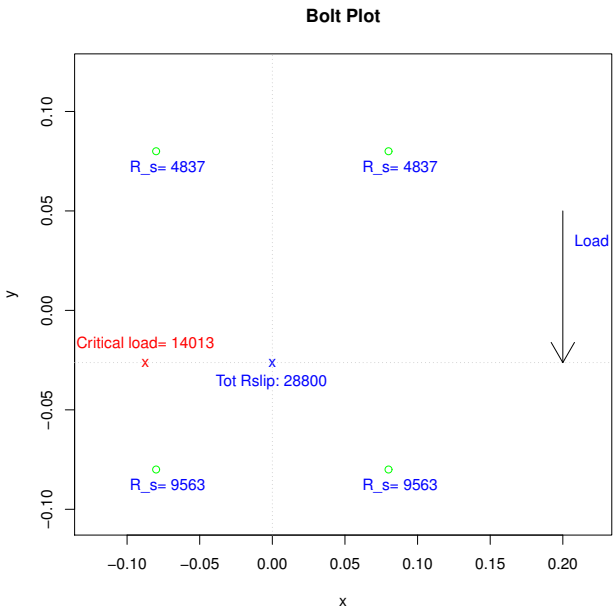

Figure A.1: *Output from boltplot script*

A.2 Parameter Studies

The developed script can be used to perform parameter studies and see what kind of effects varying parameters have according to the developed theory.

A.2.1 Worst Bolt Model Predictions

In Section 2.5 the method of determining the first bolt to slip yields critical loads that are lowered as the length of the out-of-plane moment arm is increased. As is shown this method is not good for determining joint failure and is not used further. Figure A.2 displays how the critical loads when looking at single bolts develop with increased moment arms

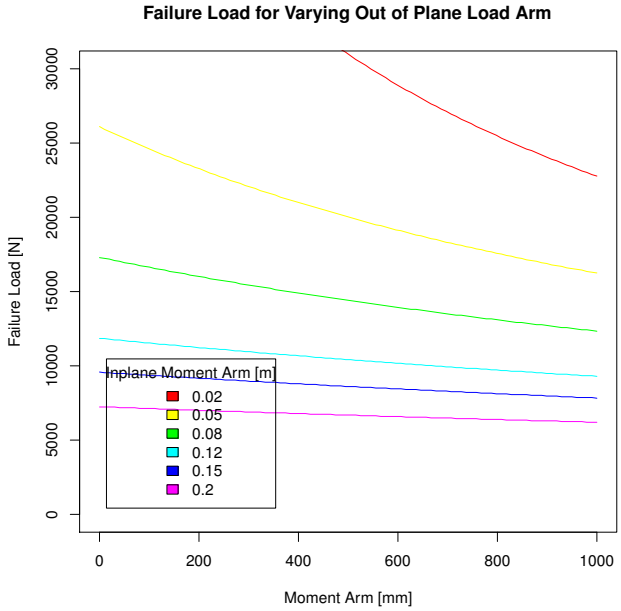

Figure A.2: *Worst Bolt Model*

A.2.2 Varying Clamped Material Stiffness

By varying the clamped material's stiffness a plot of the varying slipping loads when increasing the out-of-plane moment arm can be shown as illustrated in Figure A.3.

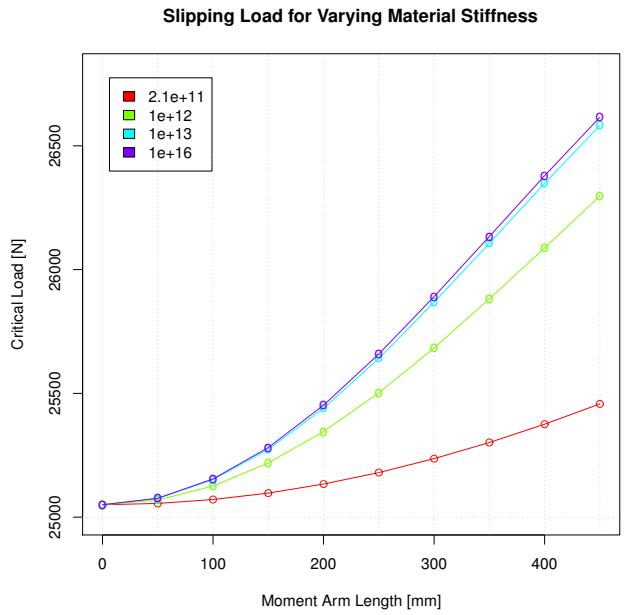

Figure A.3: *Varying material stiffness of clamped parts*

As can be seen, increasing the stiffness of the plates leads to lowered effect from the out-of-plane moment arm.

B Motivation of Rigid Body Equations

The equations used to develop the theory in this thesis has been motivated with assumptions of small deformations.

B.1 Area Moment of Inertia

The area moment of inertia chosen to calculate the bolt forces is presented in Figure B.1. This is under the assumption of small deformations. Introducing local coordinate z for the bolt and global coordinate d for the plate,

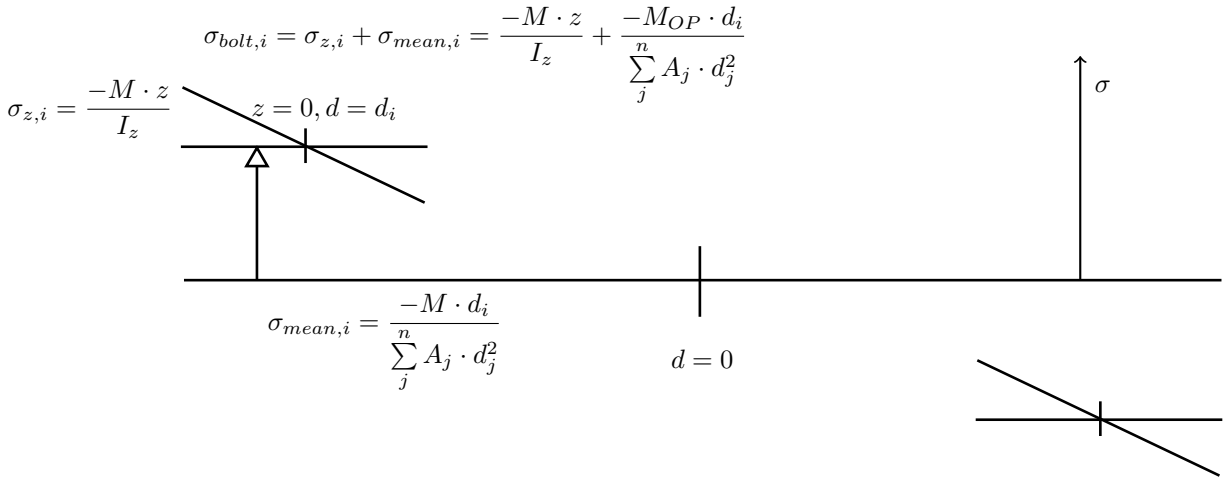

Figure B.1: *Out-of-plane moment effect on the clamped areas*

the stresses introduced by the moment can be formulated as:

$$\sigma_{mean,i} = \frac{-M \cdot d_i}{A_i \cdot d_i^2} \tag{B.1}$$

$$\sigma_{z,i} = \frac{-M \cdot z}{I_z} \tag{B.2}$$

$$\sigma_{bolt,i} = \sigma_{z,i} + \sigma_{mean,i} = \frac{-M \cdot z}{I_z} + \frac{-M_{OP} \cdot d_i}{\sum_j^n A_j \cdot d_j^2} \tag{B.3}$$

The force pertaining to the fluctuation part in Eq. (B.3) ($\sigma_{z,i}$) is then expressed as:

$$F_{z,i} = \int_A \sigma_{z,i}\, dA = \int_{-z}^{z} \frac{-M_{OP} \cdot z}{I_z} = [Antisymmetric] = 0 \tag{B.4}$$

The contribution $F_{mean,i}$ from the parallel axis theorem is computed as:

$$F_{mean,i} = \int_A \sigma_{mean,i}\, dA = \frac{-M_{OP} \cdot d_i \cdot A_i}{\sum_j^n A_j \cdot d_j^2} = \frac{-M_{OP} \cdot d_i \cdot A_i}{I_{par}} \tag{B.5}$$

Where the total force $F_{bolt,i}$ in the bolt is:

$$F_{bolt,i} = F_{z,i} + F_{mean,i} = \frac{-M_{OP} \cdot d_i \cdot A_i}{I_{par}} \tag{B.6}$$

This leads to the assumption that the only contribution to the bolt axial force is from the parallel axis theorem, this is then chosen as the area moment of inertia for the bolted plate.

B.2 Out-of-plane Moment Forces

The out-of-plane forces induced by the moment are illustrated in Figure B.2.

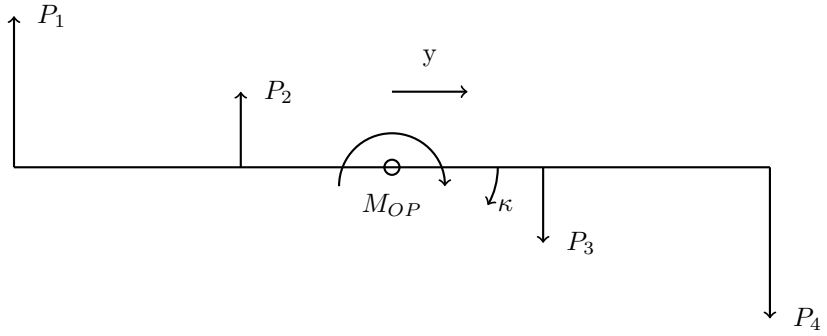

Figure B.2: *Out-of-plane moment effect on the bolts*

Where an equation for moment equilibrium can be formed as:

$$\sum_i^n P_i \cdot A_i \cdot y_i = -M_{OP} \tag{B.7}$$

A kinematic relationship between angle κ and strain ϵ_i in the bolt is given as:

$$\epsilon_i = \kappa \cdot y_i \tag{B.8}$$

Using Hooke's law:

$$P_i = E \cdot \epsilon_i = E \cdot \kappa \cdot y_i \tag{B.9}$$

Insert (B.9) into (B.7):

$$\sum_i^n E \cdot \kappa \cdot A_i \cdot y_i^2 = -M_{OP} \tag{B.10}$$

Eliminate κ:

$$\kappa = \frac{-M_{OP}}{I \cdot E}, \text{ where } I = \sum_j^n A_j \cdot d_j^2 \tag{B.11}$$

The mean pressure in the bolt is then expressed as:

$$P_i = \frac{-M_{OP} \cdot y_i}{I_{par}} \tag{B.12}$$

Where the axial force F_{OP} from the out-of-plane moment is:

$$F_{OP} = P_i \cdot A_i = \frac{-M_{OP} \cdot r_i \cdot A_i}{I_{par}} \tag{B.13}$$

B.3 In-plane Moment Forces

The kinematics for in-plane moment equilibrium is illustrated in Figure B.3.

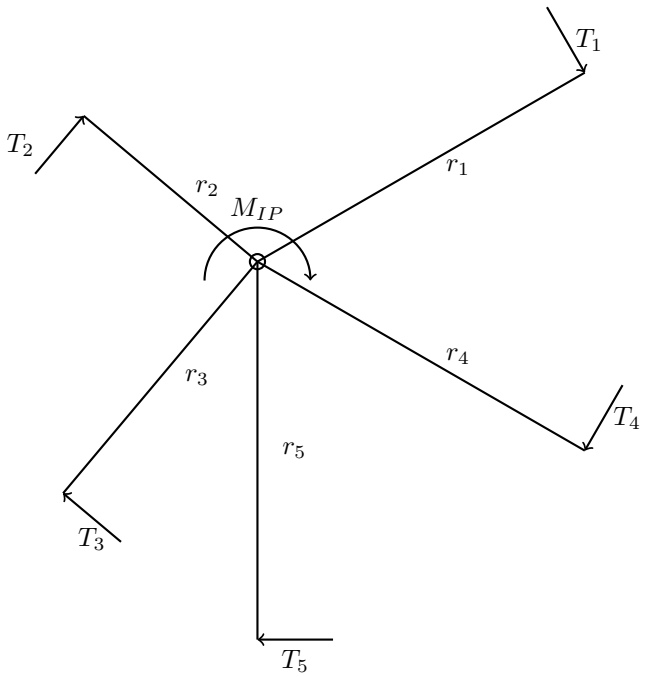

Figure B.3: *In-plane moment effect on the clamped areas*

Where an equation for moment equilibrium can be formed as:

$$\sum_i^n T_i \cdot A_i \cdot r_i = -M_{IP} \tag{B.14}$$

A kinematic relationship between angle κ and strain γ:

$$\gamma_i = \kappa \cdot r_i \tag{B.15}$$

Using Hooke's law:

$$T_i = G \cdot \gamma = G \cdot \kappa \cdot r_i \tag{B.16}$$

Insert (B.16) into (B.14):

$$\sum_i^n G \cdot \kappa \cdot A_i \cdot r_i^2 = -M_{IP} \tag{B.17}$$

G, κ are constants:

$$G \cdot \kappa \sum_i^n \cdot A_i \cdot r_i^2 = -M_{IP} \tag{B.18}$$

Eliminate κ:

$$\kappa = \frac{-M_{IP}}{I_r \cdot G}, \text{ where } I_r = \sum_j^n A_j \cdot r_j^2 \tag{B.19}$$

The mean pressure is then expressed as:

$$T_i = \frac{-M_{IP} \cdot r_i}{I_r} \tag{B.20}$$

Where the shearing force F_{IP} from the in-plane moment is:

$$F_{IP,i} = T_i \cdot A_i = \frac{-M_{IP} \cdot r_i \cdot A_i}{I_r} \tag{B.21}$$

C Automation of Post-Processing

During this project, a large number of models were run and the extraction of data from these were time consuming. Using the scripting function available in μeta, a Python script was created to automate some of the data extraction. The data collected were then compared and plotted against the theory using R. Some of the programs made is presented as source code below.

D R Code

Plot of theoretical bolt forces

```
rm(list=ls(all=TRUE))
setwd('D:/Thesis Report/Calculations')
source("sfactor.R")
setwd('D:/AloModell')
graphics.off()

# Joint Geometry
x = c(80,  80, -80, -80)*1e-3
# Changed axis of rigid body motion with 72 [mm]
y = c(80, -80, -80,  80)*1e-3+72e-3

#Read FE model results
out=readloaddata('FrameLinearBolts.csv')
arm=out$arm
```

```
Load=out$Load
Disp=out$Disp


# Pretension and Friction
F_pre=30e3
mu=0.12
E_mat=210e9
E_bolt=210e9

# Fixed moment arm
L_m=300e-3
L_p=50e-3

# Load sequence for theory
Fseq=seq(0,50e3,10e3)
F_b=matrix(0,length(x),length(Fseq))
i=1
for (F in Fseq){
  # Calculate bolt forces
  F_b[,i]=boltfor(L_m,F,F_pre,x,y,mu,E_mat,E_bolt)
  i=i+1
}
# Calculate critical loads
crit=ICcritical(x,y,L_m,L_p,F,F_pre,mu,E_mat,E_bolt)
crit=crit$crit
F_crit=boltfor(L_m,crit,F_pre,x,y,mu,E_mat,E_bolt)
print(paste(F_crit,' Newton in bolt force at critical load:',crit))
boltcol=rainbow(length(F_b[,1]))
# Plot bolt forces
for (i in 1:length(F_b[,1])){
  if (i==1)
    plot(Fseq,F_b[i,],type = "l", pch='o',col=boltcol[i], ylim=c(min(F_b),max(F_b)),xlab='Ap
  else
    matplot(Fseq,F_b[i,],type = "l",pch='o',add=1,col=boltcol[i])
}
for (i in  1:4){
matplot(Load[i,],Disp[i,],type='l',lty='dashed',add=1)
}
# Plot critical load as vertical line
abline(v=(crit), col="red", lty="solid")
abline(h=seq(10e3,50e3,1e3), col="grey", lty="dotted")
legend("topleft",inset = .05,legend=c('Theoretical','FEA'),lty=c('solid','dashed'))
# Plot critical load from FEM
FEMCRIT=27e3
abline(v=FEMCRIT, col='green', lty="solid")
text(FEMCRIT*1.25,35e3,'FEM Critical Load \n '+FEMCRIT+' [N]',col='green')
text(crit*0.7,37e3,paste('Theory Critical Load \n', format(crit,digits=5),'[N]'),col='red')
title('Bolt Forces for 300mm Moment Arm')
```

Graphical illustration of bolt positions and slip resistances together with instant centre of rotation and critical load

```
rm(list=ls(all=TRUE))
setwd('D:/Thesis_Report/Calculations')
source("sfactor.R")
graphics.off()
# Joint Geometry
x = c(80,  80, -80, -80)*1e-3
y = c(80, -80, -80,  80)*1e-3-0e-3

# Pretension and Friction
F_pre=30e3
mu=0.12
F=50e3
E_mat=210e12
E_bolt=210e9

# Fixed moment arm
L_m=450e-3
L_p=200e-3

M_OP=F*L_m
F_decom=0
for (i in 1:length(x)){
F_decom[i]= M_OP*y[i]/sum(y^2)
}

crit=ICcritical(x,y,L_m,L_p,F,F_pre,mu,E_mat,E_bolt)
sfac=sfactor(L_m,L_p,crit$crit[1],F_pre,x,y,mu,E_mat,E_bolt)
Rslips=Rslip(L_m,crit$crit[1],F_pre,x,y,mu,E_mat,E_bolt)

plot(x,y,type = "p",col = 'green', xlab = "x", ylab = "y",
main = "Bolt_Plot",
xlim=c(min(c(min(x),crit$IC[1])*1.4),max(c(max(x),crit$IC[1])*1.5,L_p*1.1))
,ylim=c(min(c(min(y),crit$IC[2])*1.3),max(c(max(y),crit$IC[2])*1.5))
)

#Text for bolt slip resistance, safety factor and axial force from OOPL
text(x+max(x)*0.1,y-max(y)*0.1,paste('R_s=',format(Rslips,digits=3)),col='blue')
#Center of Gravity for current loadarm and slip resistances
cogx=sum(x*Rslips)/sum(Rslips)
cogy=sum(y*Rslips)/sum(Rslips)
text(crit$IC[1],crit$IC[2]+0.01,paste('Critical_load=',format(crit[1],digits=3)),col='red')
#COG marking
text(cogx,cogy,'x',col='blue')
text(cogx,cogy-0.01,paste('Tot_Rslip:',format(sum(Rslips),digits=3)),col='blue')
#IC marking
matplot(crit$IC[1],crit$IC[2],type='o',pch='x',col='red',add=1)
abline(h=cogy, col="gray", lty="dotted")
abline(v=cogx, col="gray", lty="dotted")
#Load marking
text(L_p+20e-3,35e-3,'Load',col='blue')
arrows(L_p,50e-3, x1 = L_p, y1 = cogy, length = 0.25, angle = 30, code = 2, col = par("fg"),
```

Collection of functions

```
sfactor <- function(L_m,L_p,F,F_pre,x,y,mu,E_mat,E_bolt){
  #Calculates a safety factor for single bolts assuming no other bolts
   sfac=0
   n=length(y);

  M_OP=F*L_m
  M_IP=F*L_p
  F_IP=F/n

   acs=alpha(x,y)
   cosa=acs[1,]
   sina=acs[2,]
   Rslips=Rslip(L_m,F,F_pre,x,y,mu,E_mat,E_bolt)

   for (i in 1:length(x)){
     F_shear = sqrt((F_IP+M_IP*r[i]/sum(r^2)*sina[i])^2+(M_IP*r[i]/sum(r^2)*cosa[i])^2)

     sfac[i] = Rslips[i] / F_shear
   }
   return(sfac)
}

ICcritical <- function(xd,yd,L_m,L_p,F,F_pre,mu,E_mat,E_bolt){
  #Searches for the critical load and center of rotation
   x0=0
   error=2
   tol=1
   P1=0
   P2=0
   x=xd
   y=yd
   k=0
   delta=0
   while (error>tol){
     Rslips=Rslip(L_m,P1,F_pre,xd,yd,mu,E_mat,E_bolt)
     #Create new coordinate center
     cogx=sum(xd*Rslips)/sum(Rslips)
     cogy=sum(yd*Rslips)/sum(Rslips)
     if (L_p==0|L_p<(sqrt(max(x,y)^2+min(x,y)^2))*0.05){
       P1=sum(Rslips)
       x0=-cogx
       print('Warning Kulak model out of reach, assume slip in load direction without rotatio
       break
     }
     k=k+1
     x0=x0-delta
     x=xd+cogx+x0
     y=yd+cogy
     r=sqrt(y^2 + x^2)
     P1=sum(Rslips*x/r)
     P2=sum(Rslips*r)/(x0+L_p)
```

```
    error=abs(P1-P2)
    delta=(P1-P2)/sum(Rslips/r)
  }
  print(paste('loops:',k,'r0',-x0,'P1',P1,'P2',P2))
  IC=c(-(x0),cogy)
  bom=list(crit=P1,IC=IC)
  return(bom)
}


boltfor <- function(L_m,F,F_pre,x,y,mu,E_mat,E_bolt){
  #Calculates the bolt forces from the external load
  M_OP=F*L_m
  F_b=0
  for (i in 1:length(x)){
      F_decom = M_OP*y[i]/sum(y^2)
      K_b=boltstiff(E_bolt,16e-3,40e-3)
      K_c=matstiff(E_mat,20e-3,30e-3,40e-3)
      K_c2=matstiff(E_mat,20e-3,30e-3,20e-3)
      K_c=(1/K_c+1/K_c2)^-1

      dL=F_decom/(K_b+K_c)

      F_b[i] = F_pre + dL*K_b
    }
  return(F_b)
}

Rslip <- function(L_m,F,F_pre,x,y,mu,E_mat,E_bolt){
  #Calculates the slip resistance of a single bolt area
  Rslip=0
  M_OP=F*L_m
  for (i in 1:length(x)){
    F_decom = -M_OP*y[i]/sum(y^2)

    K_b=boltstiff(E_bolt,16e-3,40e-3)
    K_c=matstiff(E_mat,20e-3,30e-3,40e-3)
    K_c2=matstiff(E_mat,20e-3,30e-3,20e-3)
    K_c=(1/K_c+1/K_c2)^-1
    #Spring system elongation
    dL=F_decom/(K_b+K_c)
    F_b = F_pre + dL*K_b
    Rslip[i] = (F_pre + (F_decom*K_c/(K_b+K_c))) * mu + (F_pre - (F_decom*K_b/(K_b+K_c)))* m
  }
  return(Rslip)
}
alpha <- function(x,y){
  #Calculates the alpha values for different bolt coordinates
  sina=0
  cosa=0
  alpha=0
  extra=0
  for (i in 1:length(x)){
```

```
    if      (x[i]>=0&&y[i]>0){      # x>=0,y>0
      alpha[i]=pi/2-atan(y[i]/x[i])
      sina[i]=sin(alpha[i])
      cosa[i]=cos(alpha[i])
    }
    else if (x[i]>0&&y[i]<=0){      # x>0,y<=0
      alpha[i]=pi/2+atan(abs(y[i])/x[i])
      sina[i]=sin(alpha[i])
      cosa[i]=cos(alpha[i])
    }
    else if (x[i]<0&&y[i]<0){    # x<0,y<0
      alpha[i]=3*pi/2-atan(y[i]/x[i])
      sina[i]=sin(alpha[i])
      cosa[i]=cos(alpha[i])
    }
    else {      # x<0,y>0
      alpha[i]=3*pi/2-atan(abs(y[i])/x[i])
      sina[i]=sin(alpha[i])
      cosa[i]=cos(alpha[i])
    }
    if (x[i]==0&&y[i]==0){
      sina[i]=0
      cosa[i]=0
    }
  }
  acs=rbind(alpha,cosa,sina)
  print(alpha*180/pi)
  return(acs)
}

matstiff <- function(E,r0,r1,L){
  #Stiffness cone calculation assuming 30 degree cone angle
  alpha=30*pi/180
  stiff=(pi*E*2*r0*tan(alpha))/log(((L*tan(alpha)+r1-r0)*(r1+r0))/((L*tan(alpha)+r1+r0)*(r1-
  return(stiff)
}

boltstiff <- function(E,r1,L){
  #Function to calculate the stiffness of a bolt
  A=r1^2*pi
  stiff=A*E/L
  return(stiff)
}

readloaddata <- function(filename){
#This function loads a .csv file and exctracts the data in a special order
Loaddata=read.csv(file=filename,head=0,sep=";", fill = 0,stringsAsFactors=FALSE) # 1 column
length(Loaddata[1,])
Titles='aTitles'
Load=matrix(data = 0, nrow=(length(Loaddata[1,])/4), ncol=(length(Loaddata[,1])-2),byrow=T)
Disp=matrix(data = 0, nrow=(length(Loaddata[1,])/4), ncol=(length(Loaddata[,1])-2),byrow=T)
t=seq(1,length(Loaddata[1,]),4)
l=seq(2,length(Loaddata[1,]),4)
```

```
d=seq(4,length(Loaddata[1,]),4)
for (row in 1:(length(Loaddata[1,])/4)){
  Titles[row]=Loaddata[1,t[row]]
for (col in 3:length(Loaddata[,1])){

Load[row,col-2]=Loaddata[col,l[row]]
Disp[row,col-2]=Loaddata[col,d[row]]

}
}
Load=matrix(as.numeric(unlist(Load)),nrow=nrow(Load))
Disp=matrix(as.numeric(unlist(Disp)),nrow=nrow(Disp))
arm=as.numeric(gsub("LOP", "", Titles))
armadon=list(Load=Load,Disp=Disp,arm=arm)
return(armadon)
}
```